# Detecting anthropogenic $CO_2$ changes in the interior Atlantic Ocean between 1989 and 2005

Rik Wanninkhof,[1] Scott C. Doney,[2] John L. Bullister,[3] Naomi M. Levine,[2,4] Mark Warner,[5] and Nicolas Gruber[6]

[1]   Repeat observations along the meridional Atlantic section A16 from Iceland to 56°S show substantial changes in the total dissolved inorganic carbon (DIC) concentrations in the ocean between occupations from 1989 through 2005. The changes correspond to the expected increase in DIC driven by the uptake of anthropogenic $CO_2$ from the atmosphere, but the $\Delta$DIC is more varied and larger, in some locations, than can be explained solely by this process. Concomitant large changes in oxygen ($O_2$) suggest that processes acting on the natural carbon cycle also contribute to $\Delta$DIC. Precise partial pressure of $CO_2$ measurements suggest small but systematic increases in the bottom waters. To isolate the anthropogenic $CO_2$ component ($\Delta C_{anthro}$) from $\Delta$DIC, an extended multilinear regression approach is applied along isopycnal surfaces. This yields an average depth-integrated $\Delta C_{anthro}$ of $0.53 \pm 0.05$ mol m$^{-2}$ yr$^{-1}$ with maximum values in the temperate zones of both hemispheres and a minimum in the tropical Atlantic. A higher decadal increase in the anthropogenic $CO_2$ inventory is found for the South Atlantic compared to the North Atlantic. This anthropogenic $CO_2$ accumulation pattern is opposite to that seen for the entire Anthropocene up to the 1990s. This change could perhaps be a consequence of the reduced downward transport of anthropogenic $CO_2$ in the North Atlantic due to recent climate variability. Extrapolating the results for this section to the entire Atlantic basin (63°N to 56°S) yields an uptake of $5 \pm 1$ Pg C decade$^{-1}$, which corresponds to about 25% of the annual global ocean uptake of anthropogenic $CO_2$ during this period.

## 1.   Introduction

[2]   Changing atmospheric composition, winds, temperature, and freshwater cycling are affecting the oceans on decadal time scales, but systematic observations of resulting changes in oceanic heat and freshwater content, as well as carbon, oxygen, nutrient, and transient tracer concentrations are few. The major objective of the CLIVAR/$CO_2$ repeat hydrography program (http://ushydro.ucsd.edu/; http://www.clivar.org/carbon_hydro/) is to observe and quantify these changes throughout the water column by reoccupying select ocean transects sampled in the previous 1–2 decades as part of the Joint Global Ocean Flux Study (JGOFS) and World Ocean Circulation Experiment/World Hydrographic Programme (WOCE/WHP) [*Wallace*, 2001]. Of particular interest are changes in total dissolved inorganic carbon (DIC) inventories in response to the uptake of anthropogenic $CO_2$ by the ocean.

[3]   Such observations will serve to better determine the fate of the anthropogenic $CO_2$ emitted into the atmosphere due to human activities. These observations can provide constraints for the net carbon flux of the terrestrial biosphere [*Sarmiento and Gruber*, 2002; *Sabine et al.*, 2004; *Le Quéré et al.*, 2009]. The measurements are used to challenge and evaluate numerical ocean models employed to assess the response of the ocean to increasing atmospheric $CO_2$ levels. The models are a powerful means to investigate the impact of variability on the ocean carbon cycle and consequently DIC levels in the ocean interior [*Levine et al.*, 2008]. Most models suggest that the ocean will remain the largest sustained sink for anthropogenic $CO_2$ over the next century [*Solomon et al.*, 2007]. However, ocean models differ

---

[1]Ocean Chemistry Division, AOML, NOAA, Miami, Florida, USA.
[2]Woods Hole Oceanographic Institution, Woods Hole, Massachusetts, USA.
[3]Ocean Climate Research Division, PMEL, NOAA, Seattle, Washington, USA.
[4]Now at OEB Department, Harvard University, Cambridge, Massachusetts, USA.
[5]School of Oceanography, University of Washington, Seattle, Washington, USA.
[6]Environmental Physics, Institute of Biogeochemistry and Pollutant Dynamics, ETH Zurich, Zurich, Switzerland.
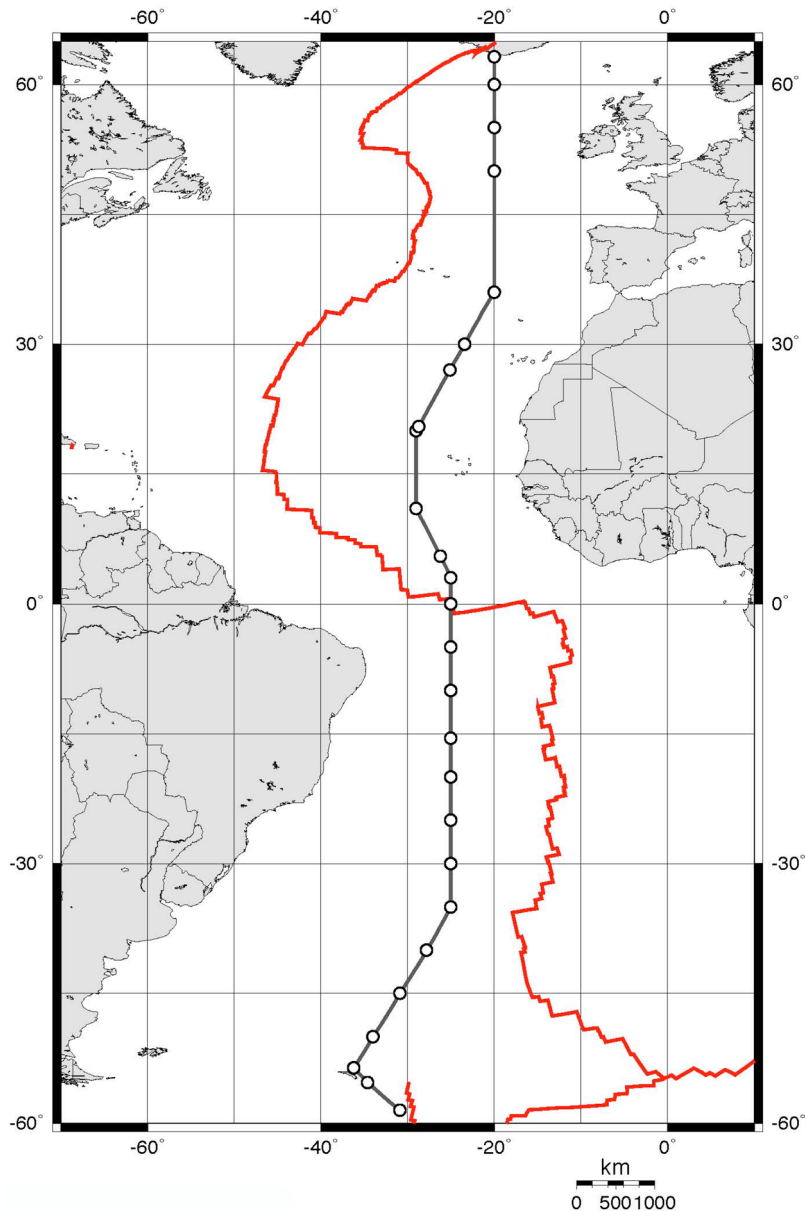
**Figure 1.** Cruise track occupied by the cruises along the A16 hydrographic transect with waypoints and 5° intervals depicted as circles. The northern section traverses the eastern basin of the North Atlantic while the southern transect (latitudes greater than 2°S) covers the western basin of the South Atlantic. The solid line shows the approximate location of the Mid-Atlantic Ridge. The SAVE 6 cruise in 1989 in the South Atlantic went to 54°S compared to 60°S for the 2005 CLIVAR/CO$_2$ reoccupation (Table 1).

appreciably in the future uptake of the ocean for different CO$_2$ emission scenarios due to different levels of uptake for a fixed climate and a given atmospheric CO$_2$ concentration, and because of changes in the oceanic carbon cycle in response to changes in climate [*Friedlingstein et al.*, 2006; *Plattner et al.*, 2008].

[4] A key question that must be addressed through observations and modeling is if there are feedbacks that will affect the uptake capacity of the ocean in response to atmospheric CO$_2$ increases and climate change [*Sarmiento and Le Quéré*, 1996; *Joos et al.*, 1999; *Lovenduski et al.*, 2007, 2008; *Le Quéré et al.*, 2007]. Therefore, sustained systematic oceanic observations are warranted [see, e.g.,

*Solomon et al.*, 2007, Figure TS.31; *Intergovernmental Oceanographic Commission*, 2009].

[5] A major accomplishment of the measurement campaigns of inorganic carbon, carbon isotopes, nutrients, and transient tracers in the ocean during the WOCE/WHP survey and the following synthesis effort was the production of a globally uniform data set, GLODAP [*Key et al.*, 2004]. This data set is used to estimate the inventory of anthropogenic carbon (C$_{anthro}$) in the ocean since the start of the industrial revolution ($\approx$ AD 1750) sometimes referred to as the Anthropocene [*Crutzen and Steffen*, 2003]. Several different independent methods converged on a total C$_{anthro}$ inventory in 1994 of 118 Petagram car-

bon (Pg C) ± 15–20% [*Sabine et al.*, 2004; *Waugh et al.*, 2006; *Khatiwala et al.*, 2009]. Appreciable differences exist between the methods for the total C$_{anthro}$ inventory for the Atlantic, with the $\Delta$C* method suggesting a total inventory of about 47 ± 7 Pg C [*Lee et al.*, 2003] for a nominal year of 1994, relatively close to that suggested by *Waugh et al.* [2006] using a Transit Time Distribution (TTD) method. *Vázquez-Rodríguez et al.* [2009] found substantially higher inventories of 54 ± 8 Pg C on average south of 65°N, on the basis of a comparison of a larger range of methods, such as the C$^0_{IPSL}$ [*Lo Monaco et al.*, 2005], TroCA [*Touratier and Goyet*, 2004], and $\varphi$C$_T$ [*Vázquez-Rodríguez et al.*, 2009] methods. However, their reported mean was driven upward primarily by the C$^0_{IPSL}$, a method that yielded a substantially higher inventory (67 Pg C) relative to the others (range of 48 to 55 Pg C). A careful assessment of the C$^0_{IPSL}$ method, such as done for the $\Delta$C* and TroCA methods [*Matsumoto and Gruber*, 2005; *Yool et al.*, 2010] will be required to constrain this number more conclusively. Nevertheless, most of the methods suggest a C$_{anthro}$ inventory for the 1990s for the Atlantic of about 50 Pg C.

[6] It is only recently that observational data on decadal changes of carbon content in the ocean have become available [*Sabine et al.*, 2004, 2008; *Peng et al.*, 2003; *Peng and Wanninkhof*, 2010; *Tanhua et al.*, 2007; *Murata et al.*, 2008; *Pérez et al.*, 2008; *Brown et al.*, 2010]. However, none of these works have estimated the decadal uptake along a meridional section for the entire Atlantic basin. Studies of changing O₂ levels in the thermocline [*Emerson et al.*, 2001; *Matear et al.*, 2000; *Johnson et al.*, 2005; *Stramma et al.*, 2008, 2010] suggest that aside from changes in DIC due to penetration of anthropogenic CO₂, appreciable additional changes in DIC are occurring on decadal time scales in the intermediate and deep waters due to changes in remineralization and ventilation rates, and water mass movement. (Note that in this manuscript we define ventilation loosely as the process by which water, which is exposed to the atmosphere, is transferred from the surface mixed layer to the interior ocean.) These decadal regional physical and biogeochemical changes are often correlated with large-scale climate reorganizations such as the El Niño–Southern Oscillation (ENSO), the Pacific Decadal Oscillation (PDO) [*Dore et al.*, 2003; *Brix et al.*, 2004; *Keeling et al.*, 2004], Southern Annular Mode (SAM) [*Lovenduski et al.*, 2007], and the North Atlantic Oscillation (NAO) [*Gruber et al.*, 2002; *Bates*, 2007; *Bates et al.*, 2002; *Thomas et al.*, 2008; *Watson et al.*, 2009; N. M. Levine et al., The impact of the North Atlantic Oscillation on the uptake and accumulation of anthropogenic CO₂ in the North Atlantic Ocean thermocline, submitted to *Global Biogeochemical Cycles*, 2010]. On smaller scales, movement of fronts, isopycnal heave, "slosh" and eddies can also cause appreciable differences in concentrations on seasonal to decadal scales [*Rodgers et al.*, 2009]. With only infrequent water column measurements, the persistence and frequency of changes can only be inferred from general knowledge of ventilation and remineralization patterns, and water mass movement. Models can aid in interpretation of signals [*Levine et al.*, 2008; *Doney et al.*, 2006; *Rodgers et al.*, 2009; *Thomas et al.*, 2008].

[7] The focus of the present study is to determine changes in DIC and C$_{anthro}$ using data obtained along the meridional A16 section between nominally 20°W and 32°W in the Atlantic Ocean from Iceland to 54°S in the Southern Ocean (Figure 1). The Atlantic Ocean is of particular interest as, compared to its size, it has disproportionately taken up more CO₂ than the other basins due to the strong meridional overturning circulation and associated deep water formation in the North Atlantic [*Lee et al.*, 2003; *Sabine et al.*, 2004]. The deep penetration of transient tracers [*Doney et al.*, 1998; *Körtzinger et al.*, 1999; *Tanhua et al.*, 2006] and C$_{anthro}$ [*Gruber*, 1998; *Lee et al.*, 2003; *Tanhua et al.*, 2007; *Vázquez-Rodríguez et al.*, 2009] in the North Atlantic compared to other basins are clear indications that uptake of anthropogenic CO₂ is controlled by water transport rather than air-sea transfer [*Sarmiento et al.*, 1992]. The current study shows that the anthropogenic CO₂ imprint is not simply a signal superimposed on a steady state background but that there is significant variability in the natural carbon cycle on decadal time scales, mostly in the upper 2000 m of the Atlantic Ocean, as manifested by variation in inorganic nutrients and O₂. The changes in nutrients and O₂ suggest changes in mixing, ventilation, and remineralization of organic carbon that will reflect in inorganic carbon levels as well.

[8] Anthropogenic CO₂ is not a property that can be directly observed, but rather must be diagnosed from DIC and other biogeochemical properties. Together with natural variability, this makes the quantification of decadal temporal trends in anthropogenic CO₂ in the ocean challenging. Thus, the inferred amount of anthropogenic CO₂ is dependent on the method of determination. The common approach for separating the anthropogenic CO₂ signal from the measured DIC assumes that there is a temporally invariant background concentration of DIC and nutrients along isopycnal surfaces that reflect the transport and mixing of "preformed" quantities. Superimposed on this background signal are concentrations of DIC and nutrients from the remineralization of organic matter and dissolution of calcium carbonates. The C$_{anthro}$ is determined as the difference between the expected change in DIC based on increases in nutrients and oxygen and measured DIC. Constant stoichiometries (Redfield ratios) between nitrate (NO$_3^-$), oxygen (O₂), and DIC are assumed to determine the remineralization component. The method was first proposed by *Brewer* [1978] and *Chen and Millero* [1979], and improved upon by *Gruber et al.* [1996]. These preformed approaches are used primarily to estimate the total anthropogenic CO₂ in the ocean, C$_{anthro}$. They have some shortcomings for estimating temporal changes in anthropogenic CO₂ over shorter intervals, $\Delta$C$_{anthro}$ [*Levine et al.*, 2008], largely because some of the underlying assumptions are not well met on shorter time scales. For example, the stoichiometric ratios may not be constant, particularly in the thermocline of the North Atlantic [*Anderson and Sarmiento*, 1994] where some of the major changes in DIC are observed. Moreover, these approaches were not designed to detect changes in the preformed DIC values caused by changes in the air-sea gas transfer and mixing into the interior as these processes do not leave a "Redfieldian" remineralization imprint. In addition, oxygen changes due to ventilation will not be correlated with those of carbon through Red-

**Table 1.** Cruises Used in the Analysis

| Cruise Name | Expo Code | Ship | Dates[a] | Extent[b] | Hydro and Bottle Data Access |
|---|---|---|---|---|---|
| SAVE 5 | 318MSAVE5 | *Melville* | 1–17 Feb 1989 | 32°S–54°S | http://cchdo.ucsd.edu/data_access?ExpoCode=318MSAVE5 |
| SAVE 6/HYDROS4 | 318MHYDROS4 | *Melville* | 21 Mar to 8 Apr 1989 | 32°S–0°S | http://cchdo.ucsd.edu/data_access?ExpoCode=318MHYDROS4 |
| OACES S.ATL-91 | 3175MB91 | *Baldrige* | 15–31 Jul 1991 | 5°N–42°S | http://www.aoml.noaa.gov/ocd/gcc/satl91.html |
| OACES N.ATL-93 | 3175MB93 | *Baldrige* | 8 Jul to 30 Aug 1993 | 5°S–64°N | http://www.aoml.noaa.gov/ocd/gcc/natl93.html |
| CLIVAR/$CO_2$ A16N | 33RO200306 | *Brown* | 19 Jun to 9 Aug 2003 | 64°N–6°S | http://cdiac.ornl.gov/oceans/RepeatSections/clivar_a16n.html |
| CLIVAR/$CO_2$ A16S | 33RO200501 | *Brown* | 17 Jan to 21 Feb 2005 | 60°S–2°S | http://cdiac.ornl.gov/oceans/RepeatSections/clivar_a16s.html |

[a]Dates are the times that ship was occupying the transect.
[b]Listed in direction of travel.

field ratios but rather through ill-constrained mechanisms of water mass mixing and differences in gas exchange response times. The inability of these preformed techniques to separate changes due to remineralization from changes due to ventilation can lead to biased estimates of $\Delta C_{anthro}$.

[9] Another approach for separating temporal changes in anthropogenic carbon from natural DIC variability is through establishing relationships between DIC and variables linked to observed changes in DIC using multilinear regressions (MLRs) [*Brewer et al.*, 1997; *Wallace*, 2001]. Applying these empirical relationships derived for the first time period to the hydrographic, nutrient, and oxygen data for the second time period and subtracting the resulting computed DIC values from the observations of DIC in the second time period yields a difference that is attributable to $\Delta C_{anthro}$. Alternatively, in an approach called the extended multilinear regression (eMLR), MLRs are created for the data sets of each of the time periods, and the two regressions are differenced to determine another estimate of $\Delta C_{anthro}$ from the hydrographic, nutrient, and oxygen data from either of the time periods [*Friis et al.*, 2005; *Tanhua et al.*, 2007]. As the eMLR method uses the observed quantities at one time as independent variables rather than the changes in the quantities between two occupations, it provides a smooth spatial pattern of anthropogenic $CO_2$ changes in the ocean compared to the MLR method that shows more spatial variability in calculated $\Delta C_{anthro}$. The MLR and eMLR methods implicitly assume that there are no appreciable temporal trends in the independent variables, and that the relationship between the dependent and independent variables remains the same except for carbon. This means that the MLR-based methods will not work over long periods when, for instance, temperature increases in the ocean will come into play, resulting in temporal changes in the different variables with a relationship that will be different than those inferred from the spatial analysis. The MLR methods are generally not used in the upper 200 to 300 m, which exhibit large seasonal changes in dependent and independent variables.

[10] Transient tracers are a good means to determine ventilation ages and ventilation pathways. The increases in trichlorofluoromethane (CFC-11) and dichlorodifluoromethane (CFC-12) in the deep and intermediate waters over time show the continued penetration of the atmospheric anthropogenic signals. However, there are limitations in using CFC-11 and CFC-12 in a quantitative sense. Mixing processes complicate the use of these tracers to determine water mass ages, although approaches such as inferring transit time distributions [*Waugh et al.*, 2006] provide a

means to better define the ages. The atmospheric source function of CFC-11 and CFC-12 are not ideal anymore for use as oceanic transient tracers as their atmospheric concentrations have stabilized and decreased after implementation of the Montreal Protocol. This results in nonunique solutions when back-calculating CFC ages from concentrations of CFC in recently ventilated water masses.

[11] However, qualitative use of these tracers in combination with other lines of evidence is a powerful means to assess the origin of changes in inorganic carbon in the Atlantic basin and to verify the different approaches to determine $\Delta C_{anthro}$. Changes in partial pressure of $CO_2$ (pCO_2) along with CFC concentrations are useful to attribute the cause in changes in DIC in the deep waters of the Atlantic Ocean where increases in DIC are near or below detection limit. CFC ages are used here as well to compare the different methods of estimating decadal changes in anthropogenic $CO_2$.

[12] Section 2 describes the Atlantic Ocean A16 cruise data that are used along with an assessment of quality and adjustments made to the data. Next, there is a description of the large-scale features in subsurface salinity, DIC, AOU, $NO_3^-$, CFC-12 age, and silicate ($SiO_2$) to show the chemical characteristics of the water masses along the meridional A16 section. This is followed by a description of temporal changes that are observed between the cruises in 1989/1993, and 2005/2003. The change in anthropogenic $CO_2$ is determined based on an eMLR approach along density surfaces, and the resulting $\Delta C_{anthro}$ is compared to the partial pressure of CFC-12 (pCFC-12). A comparison of variations of the application of the eMLR method, and back calculation methods correcting for remineralization [*Peng et al.*, 2003] to estimate $\Delta C_{anthro}$ is provided in Appendix A. The decadal $\Delta C_{anthro}$ are extrapolated for the whole basin and compared with the total anthropogenic $CO_2$ in the basin from the results of *Lee et al.* [2003] and the decadal $C_{anthro}$ changes derived from models.

## 2. Methods

[13] The cruises discussed cover a key meridional section through the Atlantic (Figure 1) with measurements of inorganic carbon parameters, transient tracers, and nutrients. Collectively, the cruises are referred to as the A16 cruises: the 1993 Ocean Atmosphere Carbon Exchange Study (OACES N.ATL-93) and the 2003 CLIVAR/$CO_2$ cruises which extend from 63°N to 2°S cover the northern section, and the 1989 South Atlantic Ventilation Experiment (SAVE 5, SAVE 6/ HYDROS4) and 2005 CLIVAR/$CO_2$ cruises are in the south (Table 1). Sampling and analysis of all parameters described

were performed following standard protocols [*World Ocean Circulation Experiment*, 1994; *U.S. Department of Energy*, 1994] using certified reference materials whenever available. The analyses for the two time periods were done with similar (and sometimes the same) instrumentation and often by the same research groups, further assuring uniformity of measurement protocol. Biases are believed to be minimal based on comparison of parameters in deep water for the cruises in 1989, 1993, 2003, and 2005. The SAVE 5 and SAVE 6/HYDROS 4 cruises in 1989 are used instead of the OACES S.ATL-91 cruise in the South Atlantic. The SAVE cruises had full water column coverage of relevant parameters at 0.5 to 1° spacing extending from the equator to 56°S, while the OACES S.ATL-91 cruise coverage had 2° spacing for the full water column, alternating with stations down to 1000 m. Moreover, the southern terminus of the OACES S.ATL-91 cruise was at 42°S. The SAVE cruises used somewhat different protocols from the later cruises and, to check for consistency, deep water carbon data from the SAVE cruises were compared with the OACES effort in 1991 over the region where the cruise tracks overlapped. No statistically significant offsets were observed in DIC for the deep water between the cruises [*Wanninkhof et al.*, 2003].

[14] The carbon, oxygen, and nutrient data of the earlier cruises (1989, 1993) were checked for consistency through extensive regional and crossover comparisons in efforts such as GLODAP [*Gouretski and Jancke*, 2000; *Key et al.*, 2004; *Wanninkhof et al.*, 2003]. The quality and offsets of CLIVAR/CO$_2$ 2003 and 2005 cruise data were scrutinized in the Carbon in the North Atlantic (CARINA) effort [*Key et al.*, 2010]. No significant offsets were determined for the data sets except for the O$_2$ and NO$_3^-$ data. The OACES N.ATL-93 O$_2$ data were systematically 7.5 $\mu$mol/kg too low [*Castle et al.*, 1998]. All O$_2$ data from the OACES N.ATL-93 cruise were corrected by this amount. We determined significant differences in deep water nitrate between the earlier (1989, 1993) and later (2003, 2005) cruises. Therefore, a correction factor of 0.996 and 0.982 was applied to all the published OACES N.ATL-93 and SAVE nitrate data, respectively, in order to reach better agreement with deep water nitrate values measured on the CLIVAR/CO$_2$ 2003 and 2005 endeavors. Phosphate data were missing for some of the earlier cruises and, therefore, PO$_4$ was not used in the analyses.

[15] Station spacing was 0.5° in latitude with samples taken at 34 to 36 depths using nominally 10 L bottles, except for the OACES N.ATL-93 cruise where stations were occupied at 1° intervals with samples taken at 24 depths. Full profiles of inorganic carbon parameters and chlorofluorocarbon (CFC) were obtained on every full-degree station, and partial profiles were taken at the half-degree stations. Oxygen, salt, and nutrient samples were obtained from every sample bottle. Vertical sample spacing ranges from 20 m in the surface mixed layer to 300 m in the deep ocean where little variability is encountered. For the 2003 and 2005 cruises, two fixed, alternating sampling depths for adjacent stations were used. For the earlier cruises, sampling was adjusted to capture specific features in the water masses. To perform comparisons between the two time periods, data were gridded on a 1° by 50 m grid with an inverse distance weighting scheme using a commercial software package (Surfer v. 7, Golden Software). This produced a gridded product that had about four times as many output values as the original chemical analyses. Close inspection suggests that the gridded products adequately represent the measurements. Maximum gridding artifacts determined from comparing measured values with the overlapping grid output were 1.4 $\mu$mol kg$^{-1}$ for DIC and 0.4 $\mu$mol kg$^{-1}$ for NO$_3^-$. The largest differences were observed in the upper thermocline where there are steep concentration gradients of chemical parameters with depth.

[16] High-quality CFC-11 and CFC-12 analyses were performed during all cruises and are used as ventilation tracers to discern pathways of penetration of atmospheric constituents into the thermocline and deep ocean. Chlorofluorocarbons are man-made with a well-defined atmospheric input history with significant releases commencing in the 1940s. CFC levels have been used to infer decadal $\Delta$C$_{anthro}$ directly [*McNeil et al.*, 2003] and the C$_{anthro}$ transient [*Khatiwala et al.*, 2009], but this requires some assumptions on uptake of CFC compared to CO$_2$. Chlorofluorocarbon levels in the water column are expressed in terms of their partial pressure or as CFC ages. The CFC-12 age provides an estimate of the time the water parcel has been isolated from the atmosphere [*Doney and Bullister*, 1992]. The method assumes that the partial pressure of CFC (pCFC) in the surface water is the same as in the atmosphere when the water is isolated from the surface. The pCFC = [CFC]/K$_0$ where [CFC] is the concentration of CFC-11 or CFC-12 in the water and K$_0$ is the solubility of CFC-11 or CFC-12 that is a function of temperature and salinity [*Warner and Weiss*, 1985]. The CFC age is determined by matching the pCFC in the water with the time the atmosphere had the same pCFC. Mixing, particularly with water devoid of CFC, biases the CFC age [*Doney et al.*, 1997]. Thus, while the CFC age should not be interpreted as an exact match of water mass age, it is an indicator of the relative age of the water. CFC-12 age and pCFC-12 are used in the analyses as they have a slightly greater dynamic range because the CFC-12 concentrations in the atmosphere stabilized later than for CFC-11.

## 3. Large-Scale Subsurface Geochemical Features

[17] The large-scale features in temperature, salinity, oxygen, and inorganic carbon along parts of this transect in the Atlantic have been described previously [e.g., *Tsuchiya et al.*, 1992, 1994; *Doney and Bullister*, 1992; *Lee et al.*, 1997; *Wanninkhof et al.*, 1999]. However, the referenced papers do not cover the entire section and do not include all parameters measured on the cruises described here, such that a brief description is provided focusing on the parameters used in the analysis. Figures 2a–2f show north-south depth profiles of salinity, AOU, DIC, NO$_3^-$, SiO$_2$, and CFC-12 age for the CLIVAR/CO$_2$ cruises in 2003 and 2005.

[18] The spatial patterns in the parameters are indicative of the large-scale water masses and transports. Near the surface, salinity is controlled by the difference in evaporation and precipitation with values exceeding 37 in the subtropics (Figure 2a). At higher latitudes, lower salinity values are encountered with a distinct asymmetry between the northern and southern latitudes. In the north, high salinity values (>35) are found well into the thermocline down to 2000 m as a result of saline waters being advected north-
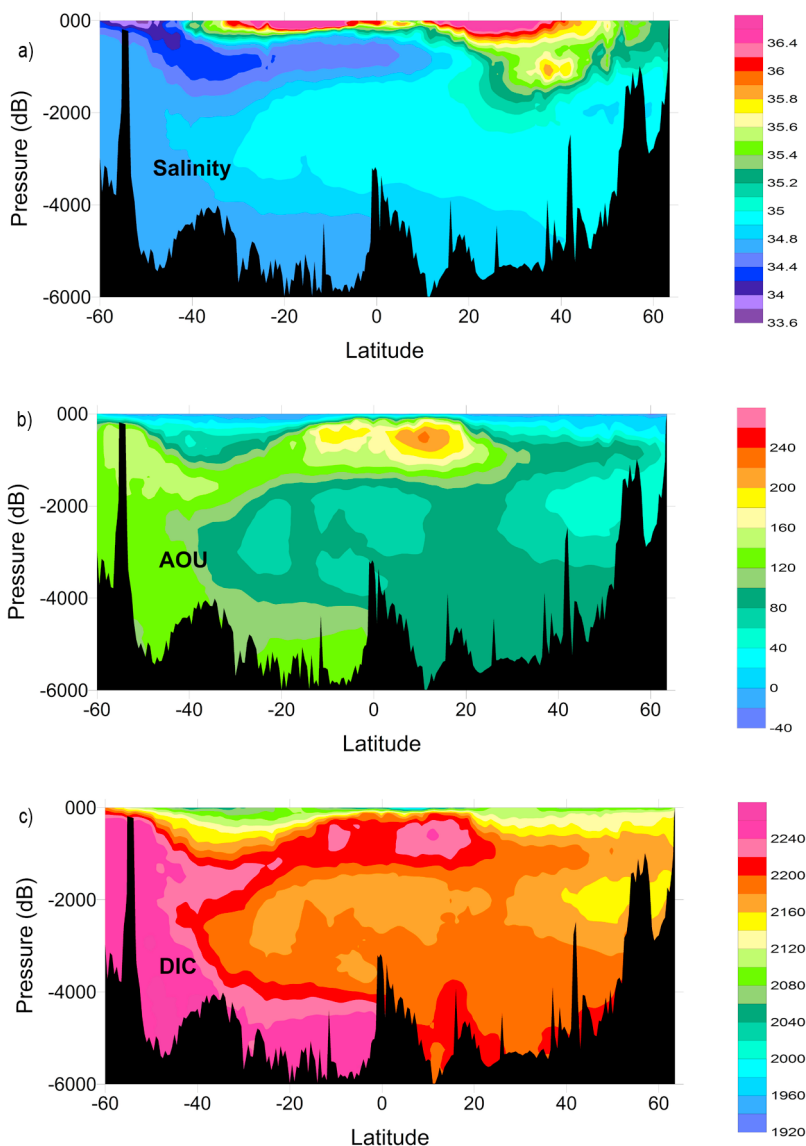
**Figure 2.** Composite cross sections (latitude versus pressure (dB)) for the 2003 and 2005 A16 cruises for (a) salinity, (b) apparent oxygen utilization (AOU in $\mu$mol kg$^{-1}$), (c) total dissolved inorganic carbon (DIC in $\mu$mol kg$^{-1}$), (d) nitrate (NO$_3^-$ in $\mu$mol kg$^{-1}$), (e) silicate (SiO$_2$ in $\mu$mol kg$^{-1}$), and (f) CFC-12 age (in years). The cutoff between the northern section, occupied in 2003, and southern section in 2005 is at 2°S.

ward by the Gulf Stream as part of the large-scale meridional overturning circulation (MOC) and the inflow of saline Mediterranean intermediate water. The return flow of the MOC in the form of North Atlantic Deep Water (NADW) is seen as water with salinities > 34.9 centered around 3000 m and is apparent as far south as 35°S. Northward transport of water originating in the Southern Hemisphere is evident as the lower-salinity water of the Antarctic Intermediate Water (AAIW) (S ≈ 34.8) centered at about 1000 m and extending to 15°N. This well-defined water mass outcrops near 45°S and has been used in the first attempts to estimate anthropogenic carbon input into the ocean [*Brewer*, 1978; *Chen and Millero*, 1979]. Antarctic bottom water (AABW) with salinities less than 34.9 lie under the NADW and its features extend as far as 40°N.

[19] The oxygen concentrations (Figure 2b) expressed as AOU are strongly affected by the large-scale transport patterns, as well as by ventilation, biological productivity, and remineralization. Low values indicate well-ventilated waters while high AOU are characteristic of waters with high remineralization and isolation from the atmosphere. The surface mixed layer shows negative AOU, indicating that O$_2$ is slightly supersaturated along the entire transect. All of the cruises occurred in the summer season, of their respective hemispheres, when near-surface oxygen supersaturation is common as a result of seasonal heating and net biological productivity producing O$_2$ [*Broecker and Peng*, 1982; *Shulenberger and Reid*, 1981], and possibly supersaturation due to bubble dissolution [*Thorpe*, 1984]. These processes exceed the rate of air-sea gas transfer of O$_2$ that
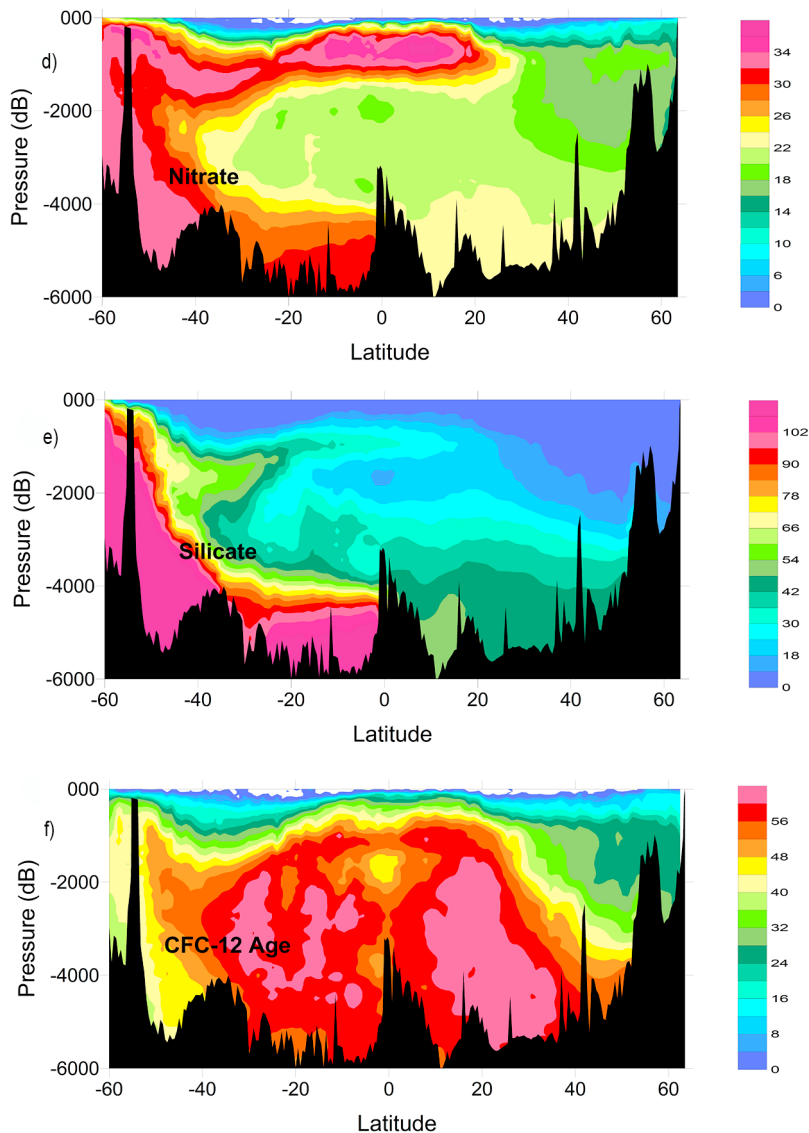
**Figure 2.** (continued)

drives the surface mixed layer toward saturation (AOU = 0). Low AOU are observed in the NADW, suggesting exposure to the atmosphere within the last couple of decades. The profiles of transient tracers [*Doney et al.*, 1998] also show recent exposure to the atmosphere. This is manifested as low CFC-12 ages in Figure 2f. The low AOU signal in the NADW shows the same extent of southern penetration as the high-salinity tongue discussed above (Figure 2a). The water of southern origin shows significantly higher AOU with the AABW having values well over 100 $\mu$mol kg$^{-1}$. The high AOU signal disappears north of the Mid-Atlantic Ridge near the equator where waters of northern origin prevail, as indicated by the large decrease in SiO$_2$ (Figure 2e). This feature is accentuated as the northern part of the transect is east of the Mid-Atlantic Ridge where there is little AABW. High AOU values are also observed in intermediate waters from 50° to 35°S immediately below the core of the AAIW,

which is the tongue of low-salinity water. The high AOU values at the northern end of the AAIW (15°S to 25°N) are caused by high biological productivity in the overlying waters and long transit time from the AAIW outcrop regions in the Southern Hemisphere. AOU with values over 220 $\mu$mol kg$^{-1}$, the highest AOU in the Atlantic basin along the A16 transect, are found at 400–700 m depth in the north tropical Atlantic due to these factors. This region also shows high NO$_3^-$ values, but it lacks a strong SiO$_2$ signal (Figures 2d and 2e).

[20] The spatial patterns in total dissolved inorganic carbon values (DIC) measured during the cruises of 2003 and 2005 (Figure 2c) are, in broad brush, similar to those of AOU, indicating that the same processes controlling AOU also affect DIC distributions. Well-ventilated waters of the NADW show low DIC despite their high salinity. The lowest subsurface DIC values are found at 1800–2000 m at high northern latitude. The two-dimensional view precludes

assigning a definitive origin of the water, but based on the hydrography of the region it is likely eastward moving water originating from the Labrador Sea and Denmark Strait area. NADW, AAIW, and AABW are delineated in the same pattern as AOU. Of note are the very high DIC values of greater than 2240 $\mu$mol kg$^{-1}$ in the undercurrents north and south of the equator at 400–700 m.

[21] The spatial distribution of NO$_3^-$ (Figure 2d) shows close similarities with those of AOU and DIC. The patterns are largely influenced by local remineralization and transport of waters with high preformed nitrate from the Southern Ocean [*Sarmiento et al.*, 2004, 2007]. The highest nitrate values are encountered at 500 m just north of the equator and are attributed to local remineralization. This can be inferred from the distribution in SiO$_2$ (Figure 2e) that does not show such maxima at these locations. Because of the slower water column remineralization of SiO$_2$, and substantial differences in the preformed values [*Sarmiento et al.*, 2007], it is a good tracer and separator of northern and southern component waters in the Atlantic [*Broecker and Peng*, 1982]. AABW has SiO$_2$ values over 100 $\mu$mol kg$^{-1}$, while NADW shows values in its core of about 20–30 $\mu$mol kg$^{-1}$.

[22] The isolation of the water masses from the atmosphere is reflected by increasing CFC-12 age with depth (Figure 2f). The oldest waters are encountered in the center of the eastern basin in the North Atlantic ($\approx$ 15–30°N) with near-zero CFC-12 concentrations (CFC-12 age > 60 years) from 2000 m to the bottom. Similar CFC ages are encountered to the south as well but not in the bottom waters due to ventilation of the AABW. The DIC, NO$_3^-$, and AOU maxima in the thermocline north and south of the equator do not correspond with the oldest CFC ages but rather have ages ranging from 30 to 50 years. This indicates that the features are heavily influenced by local remineralization rather than solely isolation.

## 4. Decadal Changes in Subsurface Water

[23] Seasonal variability is thought to have little effect on chemical parameters below the winter mixed layer, and changes in the thermocline therefore reflect primarily changes on annual to decadal scales. Rossby waves and other subseasonal perturbations contribute to the variability as well [*Rodgers et al.*, 2009]. Figures 3a–3c show changes in salinity, AOU, and DIC over time between the cruises by subtracting the gridded data of the earlier cruises from the later ones. These parameters are chosen as key biogeochemical indicators of physical, biological, and anthropogenic changes. Below the mixed layer, salinity changes are believed to be primarily a function of changes in circulation, heave and movement of fronts. AOU changes are attributed to these factors as well, but also reflect changes in ventilation and remineralization of organic matter. DIC is affected by all these processes plus increases due to the uptake of anthropogenic CO$_2$ from the atmosphere.

[24] Increases in salinity are particularly pronounced down to 1000 m at high northern latitudes (40–60°N). This is attributed to the recovery of the large salinity anomaly that occurred in the early 1990s [*Belkin*, 2004]. There is also a substantial increase in salinity over the last decade near the surface (0–400 m) from 30°S to 42°S. The areas with

decreasing salinity over the last decade are less pronounced in spatial extent. Significant decreases are observed in the North Atlantic from 5°N to 35°N down to about 500 m contrary to the longer-term trend of salinity increases from 20°N to 50°N [*Stott et al.*, 2008] and freshening of the polar and subpolar region [*Curry and Mauritzen*, 2005]. The freshening of the tropics and subtropics corresponds to an overall weakening of the NAO between 1993 and 2003 [*Stott et al.*, 2008] and the associated decreased transport of salty Gulf Stream water into the region. The intertropical convergence zone (6°N–9°N) shows large increases in salinity. The increased salinity in the intertropical convergence zone is attributed to the drought in Amazonia during 2002–2006, causing a large reduction in precipitation and river flow into the north tropical Atlantic [*Marengo et al.*, 2008].

[25] Changes in AOU are shown in Figure 3b. Most of the large differences in AOU (>|5| $\mu$mol kg$^{-1}$) are concentrated in the upper 1000 m. Large increases in AOU are seen at 700–1000 m depth from 40 to 60°N, and decreases are apparent nearer to the surface. *Johnson et al.* [2005] and *Johnson and Gruber* [2007] performed a detailed analysis of oxygen levels in the northeast Atlantic from 1988 to 2003, including the 1993 and 2003 data described here. They found that the changes are consistent with a northward movement of Mediterranean Outflow Water with high AOU since 1993 and a general contraction of the subpolar gyre. Increased ventilation of subpolar Mode Water at 0–500 m causes the observed decrease in AOU between observations. AOU increases at 500–1000 m in the region from 40 to 50°S and at 300–500 m from 16 to 20°N. There are decreases in AOU levels just north of these regions. Other areas of decrease in AOU are near the surface (50–300 m) from 5°N to 8°N and two regions of decrease in the Southern Hemisphere with one at 300–600 m centered at 8°S and the other broad region at 300–600 m from 18°S to 25°S in the subtropical gyre. While the causes of these changes are not fully understood, the trends signify appreciable decadal variability in ventilation, circulation, and biogeochemistry in the Atlantic basin in the 1990s.

[26] Changes in DIC (Figure 3c) correspond closely with the AOU anomalies (Figure 3b) but with substantially more positive anomalies in the surface water. The similarities and equal sign of the subsurface spatial patterns indicate that much of the temporal changes in DIC are related to changes in remineralization and ventilation that effect both carbon and oxygen, and shifts in water mass boundaries that act on the (natural) DIC and AOU gradients rather than on anthropogenic CO$_2$. These changes can occur by two mechanisms: (1) local increases in remineralization due to increasing rain rates of organic material or (2) changes in circulation that draws water with different AOU and DIC into the region. We disregard here the contribution of changes in the dissolution of mineral CaCO$_3$, as the relative contribution of this process to gradients in DIC is much smaller than that of organic carbon [*Gruber and Sarmiento*, 2002; *Chung et al.*, 2003]. Changes due to circulation and remineralization are difficult to separate, but models, analysis of stoichiometric ratios, and other pieces of evidence, such as CFC data, suggest that changes in ventilation and water mass movement, such as caused by heave, play a dominant role in
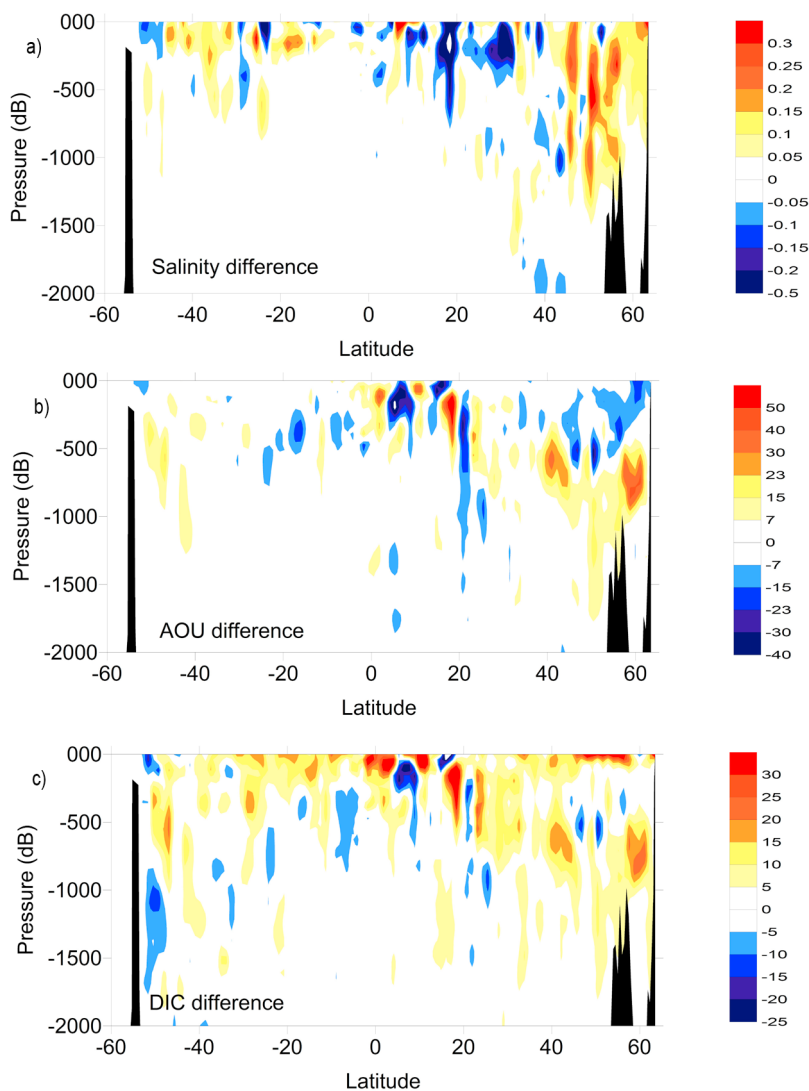
**Figure 3.** Spatial differences between repeat occupations of the A16 transect for the upper 2000 dB: (a) salinity, (b) apparent oxygen utilization ($\Delta$AOU in $\mu$mol kg$^{-1}$), and (c) total dissolved inorganic carbon ($\Delta$DIC in $\mu$mol kg$^{-1}$). For the Northern Hemisphere (60°N to 2°S) the differences are the data from 2003 minus that of 1993; for the Southern Hemisphere (2°S to 54°S) the cruises occupied the line in 2005 and 1989. The data are normalized to decadal (10 year) changes by dividing all values for the southern transect (2°S to 54°S) by 10/16 to correct for the longer time between reoccupations. The scale for $\Delta$AOU is 1.45 times that of $\Delta$DIC such that changes due to organic matter remineralization would be reflected by the same color scheme. Concentration differences near zero are blanked (see color scales).

the changes observed in DIC and AOU [*Johnson and Gruber*, 2007; *Levine et al.*, 2008; *Rodgers et al.*, 2009].

[27] Salinity anomalies also contribute to the observed differences in DIC between the two time periods. To first order, the magnitude of the changes in DIC due to freshwater dilution or concentration can be assessed though salinity normalization. The DIC values are normalized to the salinities observed in 2003/05 through: DIC$_{sal}$ = DIC · Sal$_{2003}$/Sal$_{1993}$. The maximum differences between DIC and DIC$_{sal}$ range from −20 to 20 $\mu$mol kg$^{-1}$, and the patterns correspond, of course, exactly to the salinity anomalies shown in Figure 3a. The large differences in salinity, AOU, and DIC between the time periods clearly indicate that large changes in the natural DIC pool complicate the quantification

of the $\Delta$C$_{anthro}$ signal in surface and intermediate waters, requiring sophisticated methods to separate the changes.

## 5. Deep Water Changes in DIC and pCO$_2$

[28] Decadal changes in deep water are more subtle than in the surface and intermediate waters, but detection of changes at depths below 2000 m are of relevance to estimate C$_{anthro}$ inventories by virtue of the large volume of water [*Garzoli et al.*, 2010]. It is also important to discern possible anthropogenic influences and climate change signals at depth [*Johnson and Doney*, 2006]. Current reconstructions of C$_{anthro}$ in the Atlantic based on $\Delta$C* show little penetration of C$_{anthro}$ below 2000 m, except for the North Atlantic

[*Gruber*, 1998; *Lee et al.*, 2003; *Sabine et al.*, 2004]. Other approaches show deep penetration at high southern latitudes as well [*Vázquez-Rodríguez et al.*, 2009], but these studies do not show appreciable deep water C$_{anthro}$ in the interior away from high latitudes. The deep ocean C$_{anthro}$ reconstructions are associated with substantial uncertainties, and C$_{anthro}$ estimates of less than 5 $\mu$mol kg$^{-1}$ are not considered very reliable [*Gruber et al.*, 1996]. Furthermore, *Matsumoto and Gruber* [2005] showed that there is a tendency for the $\Delta$C* method to underestimate deep ocean C$_{anthro}$ levels. Several lines of evidence suggest a penetration of C$_{anthro}$ into the deep Atlantic. *Körtzinger et al.* [1999] and *Wallace et al.* [1994] have shown measurable carbon tetrachloride CCl$_4$ in the deep Atlantic Ocean. This compound has no significant natural sources, and human emissions of CCl$_4$ started in the early 1900s compared to CFC emissions that commenced at significant quantities after 1940. While hydrolysis of CCl$_4$ and other removal mechanisms, particularly in thermocline [*Wallace et al.*, 1994], precludes its use as a robust age tracer, the presence of CCl$_4$ implies that C$_{anthro}$ has penetrated to these depths. *Johnson and Doney* [2006] detected small changes in temperature in AABW in the South Atlantic along the A16 transect over the last decade that might be due to anthropogenic climate change. *Brown et al.* [2010] using three cruises along the 24.5°W (A5) transect in 1992, 1998, and 2004 suggest small increases ($\approx$ 2 $\mu$mol kg$^{-1}$) in C$_{anthro}$ in the bottom water. *Pérez et al.* [2008] suggest similar small increases in the Irminger Sea between 1983 and 2003.

[29] With measurement uncertainties in DIC of $\pm$ 2 $\mu$mol kg$^{-1}$ and expected decadal DIC changes driven by changes in anthropogenic CO$_2$ in deep water comparable to this level, it is difficult to attribute quantitatively $\Delta$C$_{anthro}$ in deep water on decadal time scales. However, changes in DIC can be deduced from other inorganic carbon parameters, such as the subsurface partial pressure of CO$_2$, which was measured on all cruises. The partial pressure of CO$_2$ measured at 20°C, pCO$_2$(20), has about six times the dynamic range of DIC with comparable precision [*Wanninkhof and Thoning*, 1993], thereby increasing the signal-to-noise ratio substantially. While the changes in pCO$_2$(20) over time are not a unique tracer of C$_{anthro}$, since changes in remineralization will also affect pCO$_2$(20), it can provide evidence of changes that might be attributed to invasion of C$_{anthro}$ when used in concert with other tracers.

[30] Deep water $\Delta$pCO$_2$(20), which is the difference between the CLIVAR and WOCE cruise values, is shown as 4° latitude averages for sigma-4 surfaces below 45.813 kg m$^{-3}$ ($\approx$ > 3500 m), from 40°N to 40°S, in Figure 4a. The corresponding values for $\Delta$DIC and $\Delta$AOU are shown in Figures 4b and 4c, emphasizing the utility of pCO$_2$(20) for detecting changes in the deep ocean. The pCO$_2$(20) shows a consistent increase of about 10 $\mu$atm decade$^{-1}$ over the time interval between cruises along this deep section except for 12–20°N and 12–16°S. For the DIC and TAlk concentrations at these depths this corresponds to a change in DIC of 1.5 $\mu$mol kg$^{-1}$ decade$^{-1}$ at constant TAlk. The regions between 12 and 20°N show both smaller $\Delta$pCO$_2$(20) and larger variability as indicated by the larger standard error (Figure 4a) similar to the changes in $\Delta$AOU (Figure 4c). At southern latitudes greater than 32°S, the larger values of $\Delta$pCO$_2$ are consistent with the penetration pathway of the AABW, i.e., reflect younger waters relative to those further

north. The observed $\Delta$DIC for each 4° bin scatter about 0 in deep water (Figure 4b). The change in DIC corrected for changes in remineralization, $\Delta$DIC$_{O2}$ (see equation (A1) of Appendix A for the definition of $\Delta$DIC$_{O2}$), are systematically higher, suggesting a DIC increase independent of remineralization processes. However, the increase is small compared to the uncertainty in DIC measurements of about 2 $\mu$mol kg$^{-1}$. In the tropical North Atlantic ($\approx$ 0 to 24°N), the AOU values have decreased slightly, which would lead to negative changes in $\Delta$pCO$_2$ if the AOU decrease is caused by decreases in remineralization. Thus, the $\Delta$pCO$_2$ attributed to anthropogenic CO$_2$ in the tropics might actually be slightly larger than observed in Figure 4a. Attribution of the signal to anthropogenic changes cannot be definitive, as small changes in either DIC or TAlk will have a pronounced effect on the pCO$_2$(20). However, the combination of appreciable change in $\Delta$pCO$_2$(20), together with detectable pCFC, little change in AOU, and small but predominant positive changes in $\Delta$DIC$_{O2}$, suggests that decadal changes in C$_{anthro}$ are occurring in the deep waters. Table 2 provides a summary of deep water $\Delta$pCO$_2$, $\Delta$DIC$_{O2}$, $\Delta$DIC, and $\Delta$DIC$_{eMLRdens}$ (see description below) of the northern section (>15°N), the tropical, and southern sections (<15°S) along with an average of the entire section. There is a section-wide increase in $\Delta$C$_{anthro}$ of 0.4–1.3 $\mu$mol kg$^{-1}$ decade$^{-1}$ in deep water (for $\Delta$DIC$_{eMLR-dens}$ and $\Delta$DIC$_{O2}$ estimates) but with an uncertainty of over 1 $\mu$mol kg$^{-1}$ decade$^{-1}$. The $\Delta$pCO$_2$ shows an average increase of 9.3 $\mu$atm decade$^{-1}$, and the consistently positive values affirm the small increases in $\Delta$C$_{anthro}$. The northern section of the line covers the deep eastern basin, which belongs to the least ventilated deep basins of the entire Atlantic, and it correspondingly shows lower decadal changes.

## 6. Detecting Decadal Changes Due to the Invasion of Anthropogenic CO$_2$

[31] Among the many ways to estimate the change in anthropogenic CO$_2$ in the ocean, we have the greatest confidence in an approach called the extended multiple linear regression applied along isopycnal surfaces (eMLR$_{dens}$), in part because of the good correspondence with patterns of CFC penetration into the ocean. The eMLR$_{dens}$ method also tends to reduce the dynamic range of DIC values that need to be captured by the regression, reducing the absolute values of the residuals, and hence minimizing the uncertainty of the approach.

[32] Issues with the decomposition of the $\Delta$DIC signal can be minimized with an empirical multilinear regression (MLR) approach [*Wallace*, 2001], which we apply in the extended form (eMLR) as described by *Friis et al.* [2005]. For the (single) MLR, a multilinear regression is determined between DIC and a number of independent variables for time 1, t$_1$:

$$DIC_{MLR1, \, t1} = a_1 + b_1 \ SiO_{2t1} + c_1 \ NO_{3t1} + d_1 \ AOU_{t1} + e_1 \ S_{t1} + f_1 \ T_{t1}. \tag{1}$$

These coefficients, a$_1$–f$_1$, are then used with the independent variables for a later time, t$_2$, to calculate DIC at time t$_2$ (DIC$_{MLR1, \, t2}$). The difference between the observed and
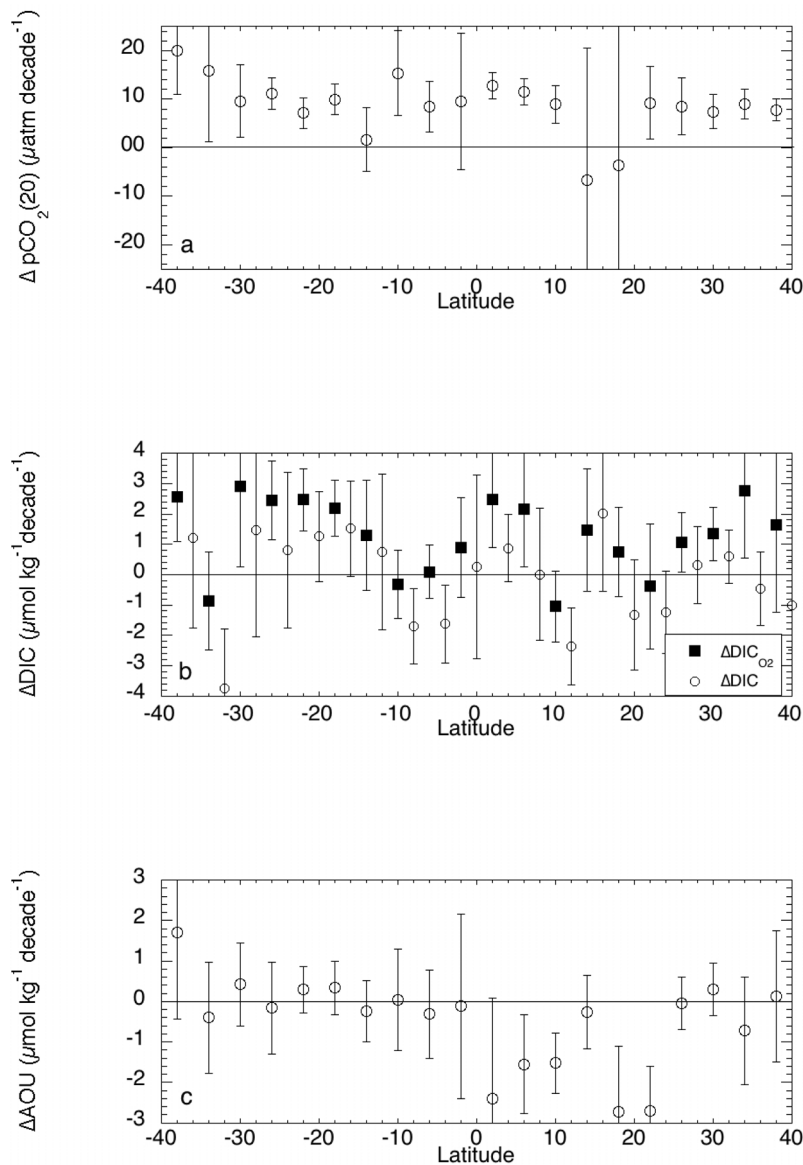
**Figure 4.** Rate of change with time in deep water biogeochemical properties along the A16 transect between 40°N and 40°S. Deep water values are averaged over 4° latitude bins, where deep water is defined as potential density anomalies referenced to 4000 dB, sigma-4, greater than 45.813 kg m$^{-3}$ corresponding with depths greater than approximately 3500 m. The error bars are the standard error for all points within the 4° interval. All changes are expressed over a decade. The differences are displayed versus latitude for (a) $\Delta pCO_2(20)$, (b) $\Delta DIC$ (open circles) and $\Delta DIC_{O2}$ (solid squares), and (c) $\Delta AOU$.

calculated DIC for time $t_2$ ($DIC_{t2}$) is assumed to be the anthropogenic $CO_2$ increase:

$$\Delta DIC_{MLR} = DIC_{t2} - DIC_{MLR1, t2} = DIC_{t2} - (a_1 + b_1 \; SiO_{2t2} \\ + c_1 \; NO_{3t2} + d_1 \; AOU_{t2} + e_1 \; S_{t2} + f_1 \; T_{t2}). \quad (2)$$

In the eMLR, a second regression is performed for time 2, $t_2$:

$$DIC_{MLR2, t2} = a_2 + b_2 \; SiO_{2t2} + c_2 \; NO_{3t2} + d_2 \; AOU_{t2} \\ + e_2 \; S_{t2} + f_2 \; T_{t2}. \quad (3)$$

$\Delta DIC_{eMLR}$ is then calculated by subtracting the DIC calculated for time $t_2$ using the $t_1$ regression parameters

($DIC_{MLR1, t2}$) from the DIC calculated for time $t_2$ using the $t_2$ regression parameters ($DIC_{MLR2, t2}$).

$$\Delta DIC_{eMLR} = DIC_{MLR2, t2} - DIC_{MLR1, t2} \\ = (a_2 - a_1) + (b_2 - b_1) \; SiO_{2t2} + (c_2 - c_1) \; NO_{3t2} \\ + (d_2 - d_1) \; AOU_{t2} + (e_2 - e_1) \; S_{t2} + (f_2 - f_1) \; T_{t2} \quad (4)$$

[33] The significance of each term is estimated from a stepwise regression of the independent parameters used in equations (1) and (3). A stepwise MLR for the whole 1991 and 1993 data set shows a decreasing ranking of importance

**Table 2.** Decadal Change in Average Deep Water (sigma-4 > 45.813) Inorganic Carbon Properties[a]

| Method | North Atlantic (>15°N) | Equatorial Atlantic (15°N–15°S) | South Atlantic (>15°S) | Full Section |
|---|---|---|---|---|
| $\Delta pCO_2(20)$ ($\mu$atm) | 6.4 (4.9) | 10.6 (9.2) | 10.8 (5.9) | 9.3 (7.5) |
| $\Delta DIC_{O2}$ ($\mu$mol kg$^{-1}$) | 1.2 (1.0) | 0.8 (1.3) | 1.9 (1.3) | 1.3 (1.2) |
| $\Delta DIC$ ($\mu$mol kg$^{-1}$) | −0.5 (0.8) | −0.6 (1.9) | 0.5 (1.9) | −0.2 (1.5) |
| $\Delta DIC_{eMLR\text{-}dens}$ ($\mu$mol kg$^{-1}$) | 0 (1.3) | 0.1 (1.1) | 0.6 (0.5) | 0.4 (1.0) |

[a]All values are averages obtained from a gridded product for sigma-4 > 45.813 ($\approx$3500 dB). The standard deviations are given in parentheses.

to the fit from $SiO_2$, $NO_3^-$, S, T, to AOU. The correlation coefficient, $r^2$, increases from 0.61 and a root mean square, rms, error of 21 $\mu$mol kg$^{-1}$ using a constant and $SiO_2$, to a $r^2$ of 0.97 with a RMS error of 5.5 $\mu$mol kg$^{-1}$ using all the parameters in equation (1). For the section occupied in 2003 and 2005, the ranking is $SiO_2$, $NO_3^-$, AOU, S, and T with the $r^2$ increasing from 0.65 with a RMS error of 21 $\mu$mol kg$^{-1}$ using a constant and $SiO_2$, to a $r^2$ of 0.98 with a RMS error of 4.5 $\mu$mol kg$^{-1}$ using all the parameters in equation (3). The difference in ranking of AOU, from the least important parameter for improving the MLR for the older data set to the third most important parameter for the newer data, is attributed to lower quality of oxygen measurements for the older data.

[34] The eMLR approach is applied along isopycnals based on the premise that this is the preferred pathway of water movement and penetration of anthropogenic $CO_2$ into the ocean [*Gruber et al.*, 1996; *Quay et al.*, 2007]. An isopycnal analysis framework also greatly damps the aliasing of natural variability caused by vertical heave [*Doney et al.*, 2007; *Levine et al.*, 2008]. Changes in biogeochemical parameters along isopycnals are mostly gradual. Coefficients for the MLR are determined for 23 isopycnal intervals along sigma-0, sigma-2, and sigma-4 surfaces using the same intervals proposed by *Gruber* [1998] and also applied by *Lee et al.* [2003] in their quantification of anthropogenic $CO_2$ in the Atlantic basin. When estimating water column changes in $\Delta C_{anthro}$, we use the depth of the isopycnal surfaces for the 2005/2003 cruises to project the density coordinates back to depth coordinates. The residuals in the MLRs range from 2 to 6 $\mu$mol kg$^{-1}$ depending on the isopycnal surface, with higher residuals near the surface and lowest at middepth in the potential density (sigma-0) range of 26.8 to 27.3 kg m$^{-3}$ (Table 3). The larger residual near the surface is attributed in part to temporal changes that are attributed to seasonal dynamics in the independent variables. In other efforts using the eMLR approach [*Friis et al.*, 2005; *Brown et al.*, 2010], the near-surface is excluded and data is extrapolated from the bottom of the winter mixed layer to the surface. However, since the eMLR is applied along isopycnals and because the cruises were performed in the same season, we believe that our approach to create a specific eMLR for the isopycnals up to the surface is preferable. For the very deep sigma-4 layers, limited data and small ranges of independent variables lead to increases in residual values. The average residual for all isopycnal surfaces between the calculated and observed DIC for the 1993/1989 data was 4.6 $\mu$mol kg$^{-1}$ while that for the 2003/2005 data was 3.3 $\mu$mol kg$^{-1}$. The difference is attributed to less precise measurements and less coverage in the earlier era. As shown in Figure 3a, significant salinity differences were observed between the reoccupations that could change the

density structure and thus impact the results of eMLR applied along isopycnals. Inspection of the changes in density structure for the isopycnal intervals used (Table 3) shows minimal changes for the two time periods in the gridded products, and the changes in depth of isopycnals have no impact in the estimated inventories.

[35] The eMLR$_{dens}$ distribution shows the expected pattern of high $\Delta C_{anthro}$ in the subtropical surface waters and deeper penetration near the outcrops, with decreasing levels toward the interior along isopycnal surfaces (Figure 5). It also shows some interleaving of higher and lower $\Delta C_{anthro}$ differences between different density layers. Of note is the lower $\Delta C_{anthro}$ of $\approx$ 2–4 $\mu$mol kg$^{-1}$ decade$^{-1}$ in the sigma-0 27.0 to 27.2 kg m$^{-3}$ interval ($\approx$ 600 m) compared to levels of $\approx$ 4–8 $\mu$mol kg$^{-1}$ decade$^{-1}$ in the density horizons above and below in the Southern Hemisphere. These patterns often show an inverse trend with AOU that was also observed in the North Atlantic in the analysis by *Friis et al.* [2005]. This lends support to the notion that the older water parcels, as suggested by higher AOU values, have lower $\Delta C_{anthro}$. The maximum near-surface values occur in the subtropical gyres due to net convergence. This is in agreement with the finding that waters with low Revelle factors hold more anthropogenic $CO_2$ [*Sabine et al.*, 2004].

[36] In Appendix A, other estimates of $\Delta C_{anthro}$ are presented based on variations of the MLR approach. A key difference with the other methods (see Figure A2) is that penetration of the $\Delta C_{anthro}$ signal in the AABW to the bottom is absent in the eMLR$_{dens}$ analysis. CFC levels are low in the AABW at depth, and appreciable $\Delta C_{anthro}$ in this water mass would not be expected. As described above, the deep water shows changes in $pCO_2(20)$ that correspond to changes of less than 2 $\mu$mol kg$^{-1}$ decade$^{-1}$ (Figure 4b and Table 2). However, it is at depth in high southern latitudes that the various methods to determine $C_{anthro}$ differ significantly as well [*Vázquez-Rodríguez et al.*, 2009], suggesting some caution in interpreting this $\Delta C_{anthro}$ signal, or absence thereof, in this region.

## 7. Comparison of $\Delta C_{anthro}$ Trends With Transient Tracers

[37] To assess the fidelity of the eMLR$_{dens}$ method of estimating $\Delta C_{anthro}$, we compare the results with chlorofluorocarbon (CFC) measurements. Changes in CFC-11 or CFC-12 could, in principle, be used to assess changes in penetration over the time period, as shown by *Doney et al.* [1998]. However, the CFC-11 and CFC-12 levels in the atmosphere have stabilized and decreased in recent years, complicating the interpretation of trends in the upper ocean over the last decade. In addition, mixing of CFCs in the ocean affects the CFC distributions in nonlinear fashion and can

**Table 3.** Coefficients of the eMLR Along Density Surfaces (eMLR$_{dens}$) (Equation (4))

| Mid | Min | Max | Temp | Salt | AOU | NO$_3^-$ | SiO$_2$ | a$_o$ | r$^{2a}$ | n$^a$ | res.$^a$ |
|---|---|---|---|---|---|---|---|---|---|---|---|
| | | | | | *Sigma Theta* | | | | | | |
| 25.3 | 25 | 25.45 | 3.326 | −2.61 | −0.153 | 1.59 | −0.920 | 33.6 | 0.92 | 100 | 5.9 |
| 25.6 | 25.45 | 25.75 | 4.999 | −11.33 | 0.073 | −1.24 | 2.067 | 317.0 | 0.96 | 65 | 5.0 |
| 25.9 | 25.75 | 26.05 | −0.771 | −3.62 | 0.104 | −0.66 | −2.788 | 159.9 | 0.98 | 77 | 4.7 |
| 26.2 | 26.05 | 26.35 | −4.731 | 9.22 | 0.334 | −2.37 | −2.267 | −234.5 | 0.99 | 126 | 3.7 |
| 26.5 | 26.35 | 26.65 | 1.688 | −5.60 | −0.095 | 0.46 | 0.385 | 183.4 | 0.99 | 270 | 3.4 |
| 26.8 | 26.65 | 26.95 | 2.044 | 1.99 | −0.236 | 2.17 | −0.683 | −99.3 | 0.99 | 349 | 4.0 |
| 27.1 | 26.95 | 27.25 | −0.210 | −5.55 | 0.072 | −1.23 | 0.472 | 214.8 | 0.99 | 563 | 4.2 |
| 27.3 | 27.25 | 27.35 | −0.644 | 9.60 | −0.109 | 0.63 | 0.006 | −331.2 | 0.99 | 173 | 2.8 |
| 27.4 | 27.35 | 27.45 | 1.185 | 5.84 | −0.130 | 0.78 | 0.193 | −218.3 | 0.99 | 190 | 2.3 |
| | | | | | *Sigma-2* | | | | | | |
| 36.45 | 36.4 | 36.5 | −6.336 | 18.23 | −0.058 | 0.21 | −0.322 | −588.2 | 0.98 | 130 | 2.8 |
| 36.55 | 36.5 | 36.6 | 2.749 | −7.44 | −0.183 | 0.83 | 0.002 | 246.6 | 0.97 | 136 | 2.6 |
| 36.65 | 36.6 | 36.7 | 4.193 | −10.48 | −0.100 | 0.62 | 0.161 | 338.9 | 0.98 | 151 | 2.9 |
| 36.75 | 36.7 | 36.8 | 6.091 | −31.87 | 0.015 | −1.30 | 0.383 | 1107.1 | 0.99 | 146 | 2.4 |
| 36.85 | 36.8 | 36.9 | 1.565 | −3.90 | −0.123 | −0.03 | 0.204 | 137.0 | 0.99 | 206 | 2.4 |
| 36.95 | 36.9 | 36.98 | 6.868 | −24.99 | −0.206 | 0.03 | 0.392 | 856.6 | 0.99 | 232 | 2.8 |
| 37.00 | 36.98 | 37.03 | 9.364 | −71.16 | −0.111 | −0.99 | 0.325 | 2478.8 | 0.99 | 197 | 3.0 |
| 37.05 | 37.03 | 37.08 | 7.608 | −95.09 | −0.085 | −0.10 | −0.019 | 3312.2 | 0.98 | 298 | 3.3 |
| | | | | | *Sigma-4* | | | | | | |
| 45.825 | 45.813 | 45.838 | 8.049 | −94.39 | −0.624 | 3.53 | 0.045 | 3252.4 | 0.97 | 86 | 3.7 |
| 45.85 | 45.838 | 45.863 | −4.490 | −63.72 | 0.188 | −1.01 | −0.273 | 2250.9 | 0.98 | 106 | 3.3 |
| 45.875 | 45.863 | 45.888 | −2.377 | 18.77 | −0.229 | 4.55 | −0.453 | −709.7 | 0.99 | 110 | 2.3 |
| 45.9 | 45.888 | 45.913 | −11.646 | 405.51 | −0.331 | −3.31 | 1.813 | −14108.8 | 0.98 | 44 | 3.5 |
| 45.925 | 45.913 | 45.938 | 16.281 | 31.71 | −0.341 | −0.63 | 0.773 | −1132.4 | 0.99 | 28 | 1.8 |
| 45.95 | 45.938 | 45.963 | 64.693 | −425.02 | −1.104 | 0.29 | 0.690 | 14768.4 | 0.99 | 69 | 2.1 |

[a]The count (n), correlation coefficient (r$^2$), and residual (res.) are those determined for the respective MLRs derived from 2003/2005 data. No straightforward error statistics can be derived for the eMLR compared to the single MLR (see text, *Friis et al.* [2005], *Tanhua et al.* [2007], and *Levine et al.* [2008]).

have a significant effect on the interpretation of differences between time periods [*Waugh et al.*, 2006]. As a result, no strong correlations are found between changes in CFC over the time period and $\Delta C_{anthro}$. However, there are characteristic trends between $\Delta C_{anthro}$ and pCFC that are diagnostic.

[38] The comparison between $\Delta C_{anthro}$ and CFC concentrations is done in terms of partial pressure of CFC-12, pCFC-12, to avoid misrepresentation due to the solubility dependence of CFC concentrations. Figure 6 shows the trends of $\Delta DIC_{eMLRdens}$, which is the $\Delta C_{anthro}$ calculated by the eMLR applied along isopycnals, versus pCFC-12 for the depth range of 250–2500 dB. There is a general increase in $\Delta C_{anthro}$ with increasing pCFC-12 but with significant scatter that is attributed to several factors: the time histories of pCFC and anthropogenic CO$_2$ in the atmosphere are different, with the pCFC-12 increases occurring over a
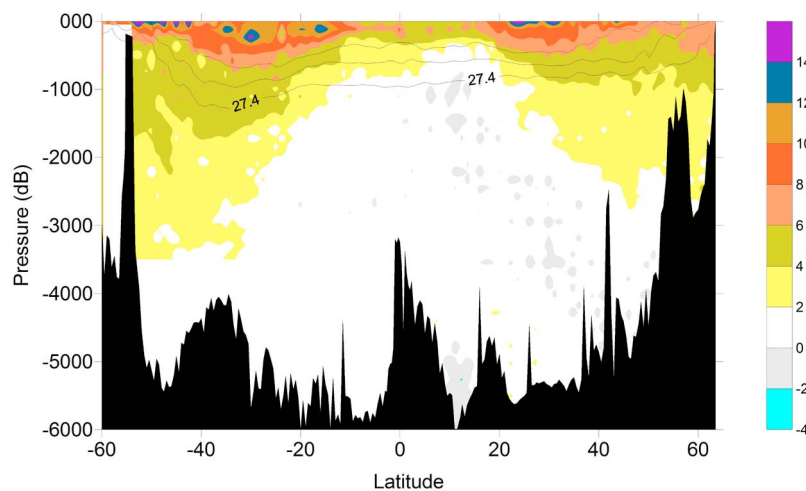


**Figure 5.** The change in anthropogenic carbon, $\Delta C_{anthro}$, for the time interval between cruises along the A16 transect estimated by the extended multilinear regression (eMLR) method with separate multilinear regressions (MLRs) determined for each of 23 distinct density ranges (Table 3). The eMLR based change in anthropogenic carbon, $\Delta DIC_{eMLRdens}$, is computed utilizing S, T, AOU, NO$_3^-$, and SiO$_2$ from 2003/2005 as input parameters. The solid lines indicate potential density horizons, sigma-0 = 27.0, 27.2, and 27.4 kg m$^{-3}$.
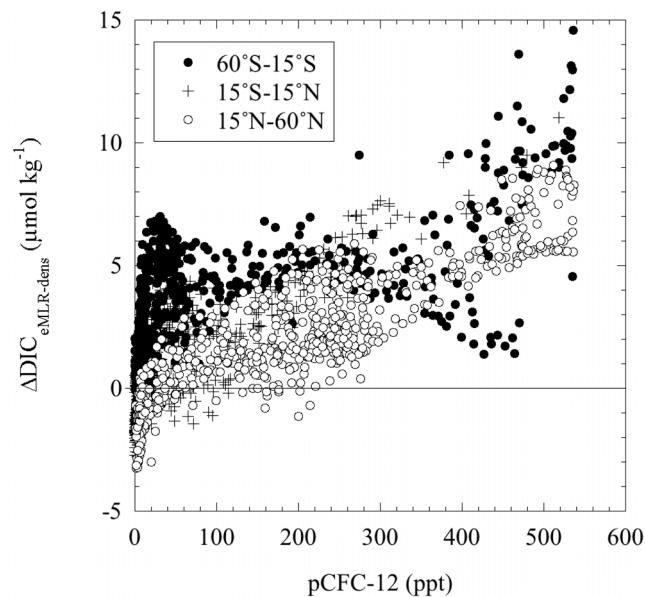
**Figure 6.** The eMLR based change in anthropogenic carbon, $\Delta DIC_{eMLRdens}$, versus pCFC-12 determined from the CLIVAR/CO$_2$ cruises in 2003 and 2005 for the pressure range of 200–2500 dB. The solid circles are for samples from 60°S to 15°S, the plus symbols are those from 15°S to 15°N, and the open circles are those from 15°N to 60°N. For clarity, only 1/3 of the data points for the 60°S to 15°S and 15°N to 60°N intervals are plotted.

much shorter period starting after about 1945 with a rapid increase till the mid-1980s and stabilizing in the mid-1990s. In comparison, the atmospheric CO$_2$ growth rate has increased monotonically over this time period such that mixing of water will cause a nonunique pattern of $\Delta C_{anthro}$ and pCFC-12. The rapid increase of $\Delta C_{anthro}$ at low pCFC-12 in Figure 6 is attributed to mixing of water containing $\Delta C_{anthro}$ and pCFC-12 with older water that is free of CFC but contains appreciable anthropogenic CO$_2$. To highlight the different trends in the Atlantic basin, the data are separated in regions poleward of 15°N and 15°S and the tropical area. The $\Delta DIC_{eMLRdens}$ (Figure 6) shows a rapid increase of anthropogenic CO$_2$ at low pCFC-12 ($\approx$ 0–80 ppt) in the Southern Hemisphere that is attributed to mixing of older waters as described above. The southern waters show slightly greater $\Delta C_{anthro}$ for a given pCFC than the northern section except for CFC-12 values between 300 and 500 ppt, which are associated with shallow AABW. The trends in the Southern Hemisphere suggest a complicated mixing and penetration pattern of anthropogenic CO$_2$.

[39] The northern section trend is more homogeneous and is attributed to more rapid mixing along the isopycnals [*Doney and Bullister*, 1992; *Doney et al.*, 1997]. The negative $\Delta DIC_{eMLRdens}$ in the interior of the northern section suggests that the eMLR$_{dens}$ technique does not fully capture $\Delta C_{anthro}$, as no systematic negative $\Delta C_{anthro}$ values would be expected with the eMLR approach. Thus, the water column inventory might be underestimated at low latitudes. The equatorial area shows both patterns of Northern and Southern Hemispheres because waters from northern and

southern origins impact the region. The maximum values of $\Delta DIC_{eMLRdens}$ agree with expected net increases in $\Delta C_{anthro}$ in surface water of 6–10 $\mu$mol kg$^{-1}$ decade$^{-1}$ if the DIC in surface water keeps up with atmospheric CO$_2$ increases. The other approaches to determine $\Delta C_{anthro}$ discussed in Appendix A show trends with pCFC-12 and $\Delta C_{anthro}$ that differ from what would be expected based on their atmospheric input histories (see Figure A4).

[40] To further assess the fidelity of the $\Delta DIC_{eMLRdens}$ method, we show the spatial distribution of this parameter along with other diagnostics on a sigma-0 surface of 27.3 kg m$^{-3}$ in Figure 7. This isopycnal surface of AAIW outcrops at high latitudes, reaches a maximum depth of 1100 m in the South Atlantic subtropical gyre, and continues at 700–800 m depth in the North Atlantic up to 45°N where it shoals rapidly (Figure 7a, right axis). CFC-12 ages (Figure 7a, left axis) show a progressive aging from high latitude to a maximum tracer age of 55 years at 10°N and 10°S. Given the CFC-12 atmospheric time history, computed CFC-12 tracer ages have a maximum bound of about 60 years, and the actual mean ages along this isopycnal in the tropics are likely higher. Along the equator there appears to be some ventilation and/or mixing, with ages decreasing to 45 years likely due to the zonal undercurrents in this region. The DIC values (Figure 7b) for the 2003/2005 data progressively increase along the isopycnal toward the tropics, due to re-mineralization, with an increase of 110 $\mu$mol kg$^{-1}$ in the northern tropical region and 70 $\mu$mol kg$^{-1}$ in the southern tropical region compared to the southern outcrop region. It is of note that the DIC calculated from MLR$_{dens}$ created from the 2003/2005 data (equation 3) reproduce the observed DIC values very closely (Figure 7b). Figure 7b shows the challenge of estimating $\Delta C_{anthro}$ (<10 $\mu$mol kg$^{-1}$ decade$^{-1}$) superimposed on a large spatial range of DIC ($\approx$ 50–100 $\mu$mol kg$^{-1}$). The $\Delta DIC_{eMLRdens}$ with coefficients specific to this density horizon (Table 3) shows larger changes nearer to the outcrop areas and spatial patterns roughly inverse to those of CFC ages (see Figure 7a). However, the $\Delta DIC_{eMLRdens}$ values go negative for the oldest waters. There is a sharp salinity gradient along this isopycnal around 20–15°N, indicating a transition from warmer and saltier northern component water to older, colder, and fresher southern component water [*Broecker and Östlund*, 1979; *Kawase and Sarmiento*, 1985] that is also reflected by a rapid increase in CFC age (Figure 7a). The density class in this region is likely formed by mixing of several different water masses that cannot be effectively captured by the eMLR$_{dens}$ method. This region also shows an increase of $\approx$ 4 $\mu$mol kg$^{-1}$ decade$^{-1}$ in AOU [*Stramma et al.*, 2010], suggesting large biogeochemical changes that could impact the eMLR results. Overall, the eMLR$_{dens}$ approach provides an estimate of $\Delta C_{anthro}$ that is consistent with patterns of ventilation and magnitude, but regional biases are apparent.

## 8. Estimate of Total Inventory Change in the Atlantic Ocean

[41] Estimates of decadal inventory changes of $\Delta C_{anthro}$ in ocean basins are few because of limited reoccupations to date, natural variability, and methodological challenges. The observations along the A16 line are believed to offer a
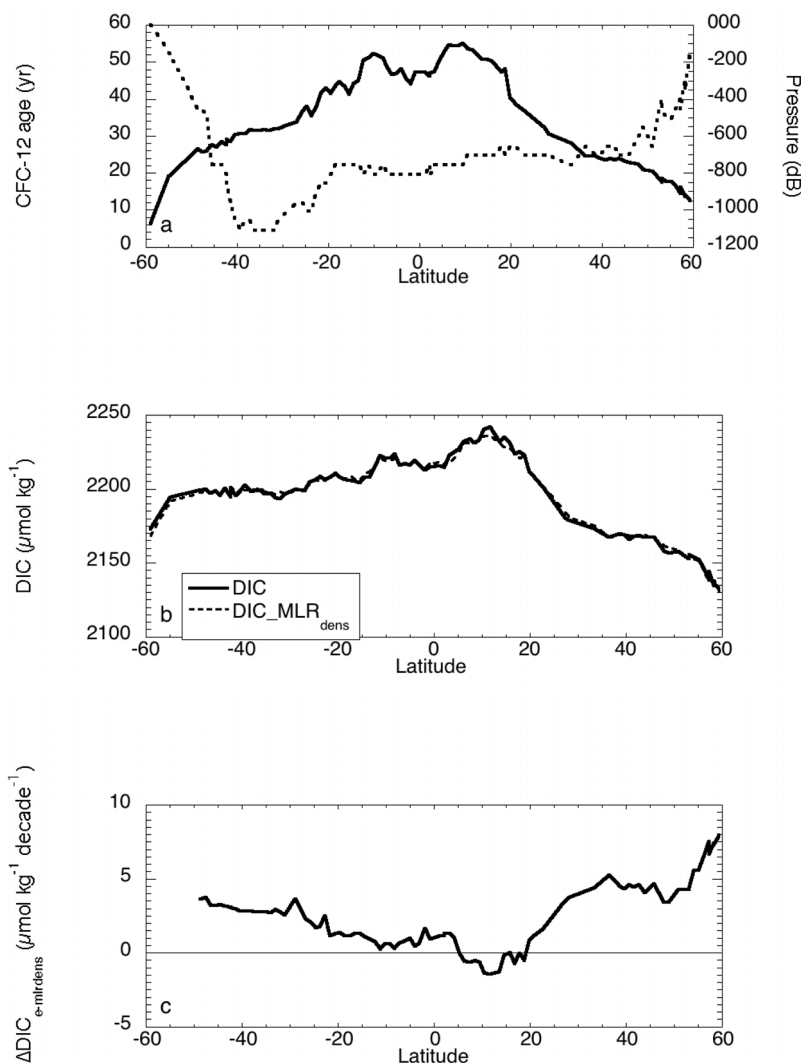
**Figure 7.** Depth, CFC-12 age, DIC, and $\Delta DIC_{eMLRdens}$ versus latitude along potential density surface, sigma-0 = 27.3 kg m$^{-3}$ using 2003/2005 data. (a) Depth of isopycnal surface 27.3 kg m$^{-3}$ (dashed line, right axis) and CFC-12 age (solid line, left axis); (b) DIC (solid line), and DIC determined from the MLR technique for the 27.25–27.35 kg m$^{-3}$ interval, MLR$_{dens}$ (dashed line); and (c) $\Delta DIC_{eMLRdens}$ normalized to a decade.

reasonable whole basin estimate for the Atlantic as it transects the middle of the basin. As shown by *Gruber et al.* [1996], *Körtzinger et al.* [1999], *Tanhua et al.* [2006], *Vázquez-Rodríguez et al.* [2009], and *Brown et al.* [2010], the C$_{anthro}$ signal penetrates deeper in the western basin of the North Atlantic compared to the eastern side, with the location of the A16 transect providing an approximate centerline. *Murata et al.* [2008] shows higher decadal changes from 1994 to 2003 in the western basin than the eastern basin of the South Atlantic (30°S). The average specific inventory trend between 35°W and 15°W obtained by *Murata et al.* [2008] was 0.71 mol m$^{-2}$ yr$^{-1}$ in agreement with our $\Delta DIC_{eMLRdens}$ estimate in the South Atlantic (>15°S) of 0.76 mol m$^{-2}$ yr$^{-1}$ (Table A1). Their zonal estimate for 30°S is 0.6 mol m$^{-2}$ yr$^{-1}$. The comprehensive analysis by *Lee et al.* [2003] of the total inventory of C$_{anthro}$ in the Atlantic, utilizing 17 cruises occupied during the

WOCE/WHP, shows that the observations along the A16 line are representative of the basin average for the total increase of C$_{anthro}$ during the Anthropocene.

[42] Extrapolating the eMLR$_{dens}$ results from A16 using a volume weighted average and integrating over depth leads to a total basin inventory change of 1.9 Pg C for the North Atlantic from 1993 to 2003 (63°N–2°S), or 1.9 Pg C decade$^{-1}$, and 5.2 Pg C for the South Atlantic (54°S–2°S) for 1989–2005, or 3.0 Pg C decade$^{-1}$. Figure 8 shows a similar decadal uptake pattern over 10° latitude bands using the eMLR$_{dens}$ method compared to the total inventory for the Anthropocene as determined by *Lee et al.* [2003]. The inventory estimates from the eMLR$_{dens}$ approach show small inventory changes at low latitude and even negative inventory changes over the decade at 16°N. This is likely an artifact of the approach as described above in that the eMLR$_{dens}$ approach does not adequately capture the
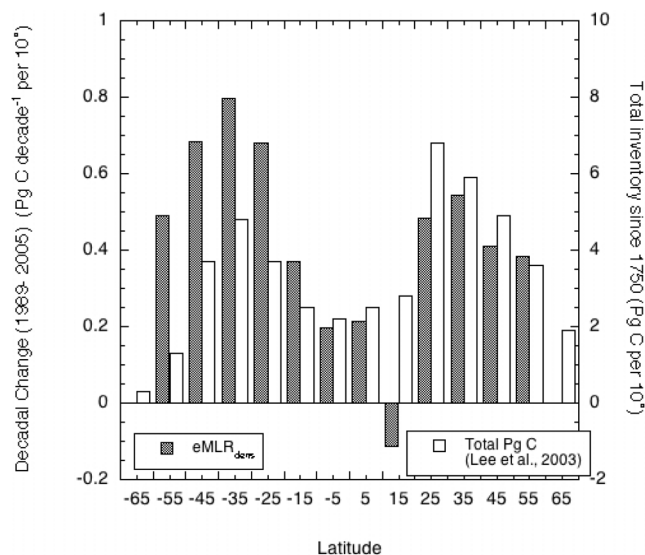
**Figure 8.** Vertically integrated decadal change of anthropogenic carbon ($\Delta C_{anthro}$) summed over 10° latitude bands along the A16 transect based on the $eMLR_{dens}$ approach (gray hatched columns), compared to the column inventory of $C_{anthro}$ (i.e., the total uptake over the Anthropocene) as determined by *Lee et al.* [2003] (white columns, right axis).

$\Delta C_{anthro}$ across fronts and mixing of water masses, as well as decadal trends of AOU in the region [*Stramma et al.*, 2010].

[43] Assessing a robust error estimate is difficult due to a variety of systematic, compensating, and random errors involved in the assumptions and extrapolations. The residuals in the eMLR are 50 to 200% of the signal (Table 3) but these are random and Gaussian, and the standard error (defined as RMS residual/(number of points)$^{0.5}$) is an order of magnitude smaller for the isopycnals where most of the change in inventory occurs. An estimate of the error for the entire basin is obtained by comparing results of different approaches. The different MLR approaches summarized in Table A1 yield a specific inventory standard deviation along the section of 0.06 mol m$^{-2}$ yr$^{-1}$ (with a mean of 0.6 mol m$^{-2}$ yr$^{-1}$) or about 10%. Following the analysis of *Lee et al.* [2003], we double the uncertainty estimate, to include the uncertainties in the basin-wide extrapolation based on the uncertainty of $C_{anthro}$ distribution, to a 20% overall uncertainty (1-sigma) or 1 Pg C decade$^{-1}$.

[44] The data-based inventory change compares well with model estimates. The basin-scale uptake of 5 ± 1 Pg C decade$^{-1}$ for the last decade is similar to $\Delta C_{anthro}$ from the CCSM BEC model [*Doney et al.*, 2009] for the Atlantic Ocean north of 64°S of 4.5 Pg C decade$^{-1}$ for the period from 1993 to 2003. Using a suite of 10 ocean general circulation models, *Mikaloff Fletcher et al.* [2006] estimate an inventory trend of 0.58 ± 0.1 Pg C yr$^{-1}$ (5.8 ± 1.0 Pg C decade$^{-1}$) for a nominal year of 1995. The estimate is based on an inversion of the $\Delta C^*$ inferred inventory of $C_{anthro}$ using the transport models to determine the magnitude and distribution of the surface fluxes of $C_{anthro}$ that are optimally consistent with that inventory.

[45] A robust feature in our estimate that is not observed in model output is that the change in the $\Delta C_{anthro}$ inventory in the South Atlantic of 3.0 Pg C decade$^{-1}$ is greater than in the North Atlantic of 1.9 Pg C decade$^{-1}$. This shows up in all of the MLR methods (see Table A1). The difference shows up in the specific inventory change as well, and thus is not solely due to a difference in volume between the North and South Atlantic, with the South Atlantic containing 56% of the total basin water volume. The greater decadal change in the inventory of anthropogenic CO₂ in the South Atlantic is opposite from the hemispheric difference in the total inventory of $C_{anthro}$ over the Anthropocene, for which 60% is found in the North Atlantic (Figure 8). The CCSM BEC model shows an even larger asymmetry with an uptake in the North Atlantic of 3.4 Pg C decade$^{-1}$ and for the South Atlantic 1.1 Pg C decade$^{-1}$ from 1993 to 2003. Our results also differ from the ocean inversion results of *Mikaloff Fletcher et al.* [2006], which also suggest an about equal distribution of anthropogenic CO₂ uptake between the North and South Atlantic (2.9 ± 0.8 Pg C yr$^{-1}$ for the region from 58°S to the equator and 3.0 ± 0.7 Pg C yr$^{-1}$ from the equator to 76°N). The result is intriguing, particularly when combined with the observation of *Quay et al.* [2007] based on $^{13}$C isotopic evidence that a significant fraction of $C_{anthro}$ in the North Atlantic is transported from the south as opposed to supplied by local air-sea gas transfer, a feature that is found only to a much smaller degree in the inversion results of *Mikaloff Fletcher et al.* [2006].

[46] This observation-based estimate suggests that the anthropogenic CO₂ uptake in the North Atlantic in the 1990s was less than the South Atlantic. Some of the difference could be because the observations were taken in the more poorly ventilated eastern basin in the North and better ventilated western basin in the South. However, the east-west asymmetry in tracers and $C_{anthro}$ as observed by *Körtzinger et al.* [1999], *Tanhua et al.* [2006], and *Brown et al.* [2010] in the North Atlantic, and by *Murata et al.* [2008] in the South Atlantic is not large enough to account for differences determined. Another important caveat is that the inventory change in the North Atlantic is from 1993 to 2003, while the South Atlantic inventory change is determined from 1989 to 2005. As shown by *Brown et al.* [2010] and *Pérez et al.* [2008], there are appreciable differences in observed $C_{anthro}$ inventory changes on subdecadal time scales in the North Atlantic.

[47] While speculative, the intensification of winds in the Southern Ocean causing upwelling of older waters leading to greater $C_{anthro}$ uptake [*Lovenduski et al.*, 2008] and decreases in meridional overturning in the North Atlantic associated with a shift in the NAO in the mid 1990s [*Thomas et al.*, 2008; Levine et al., submitted manuscript, 2010] could both be factors resulting in increasing accumulation of $C_{anthro}$ in the South Atlantic compared to the North Atlantic.

## 9. Conclusions

[48] The CLIVAR/CO₂ repeat occupation of the WOCE/WHP line A16 shows significant water column changes in O₂ and DIC, particularly in intermediate waters, compared to cruises a decade earlier. The depth of the anomalies rule out seasonal variability. The $eMLR_{dens}$ method of estimating

decadal changes in anthropogenic CO$_2$ in the water column yields a result of $0.53 \pm 0.05$ mol m$^{-2}$ yr$^{-1}$ when integrated over the entire section. When extrapolated over the basin, the eMLR$_{dens}$ method yields an anthropogenic CO$_2$ increase of $5 \pm 1$ Pg C per decade from 63°N to 56°S, consistent with recent model results. The rate of accumulation of C$_{anthro}$ is larger in the South Atlantic compared to the North Atlantic, which could be caused by recent patterns of climate variability and changes that alter the rate of transport of C$_{anthro}$ from the surface ocean into the ocean's interior. The small changes in pCFC and pCO$_2$ in deep water taken a decade apart suggest that the anthropogenic CO$_2$ signal is penetrating into the bottom waters (>3500 m) along this section. The pCFC-12 patterns are consistent with the depth distributions and regional patterns in $\Delta$C$_{anthro}$ derived using the eMLR$_{dens}$ approach.

## Appendix A: Other Approaches to Estimate $\Delta$C$_{anthro}$ and Shortcomings

[49] Here we compare several other approaches and permutations of the multiple linear regression MLR method to estimate temporal changes in ocean anthropogenic carbon $\Delta$C$_{anthro}$. This comparison is performed to show the significant differences between approaches, which are larger at regional scale than when integrated over the entire Atlantic basin, suggesting that the biases in the methods partially cancel out over larger areas. First we describe the approaches based on correcting for changes in remineralization followed by empirical multilinear regression methods.

[50] One approach for estimating $\Delta$C$_{anthro}$ is to correct the observed changes in DIC, $\Delta$DIC, for variations in organic remineralization using either AOU or NO$_3^-$, and CaCO$_3$ remineralization, using total alkalinity TAlk, and their stoichiometric (Redfield) ratios [*Peng et al.*, 2003]. The resulting $\Delta$C$_{anthro}$ estimates are denoted as $\Delta$DIC$_{O2}$ and $\Delta$DIC$_{NO3}$. The inferred change due to anthropogenic CO$_2$ input, $\Delta$C$_{anthro}$, over the period for this method is:

$$\Delta DIC_{O2} = \Delta DIC - R_{C:O}\, \Delta\, O_2 - 0.5(\Delta TAlk + R_{N:O}\, \Delta O_2)$$

$$(A1)$$

and:

$$\Delta DIC_{NO3} = \Delta DIC - R_{C:N}\, \Delta\, NO_3^- - 0.5\big(\Delta TAlk + \Delta NO_3^-\big)$$

$$(A2)$$

where $\Delta DIC = DIC_{t2} - DIC_{t1}$, $t_1$ and $t_2$ are the earlier and later time periods, respectively, and $\Delta O_2$, $\Delta NO_3^-$, and $\Delta TAlk$ are defined in the same manner. R$_{C:O}$, R$_{N:O}$, and R$_{C:N}$ are the stoichiometric (Redfield) ratios of carbon and oxygen, nitrate and oxygen, and carbon and nitrate, respectively. The stoichiometric ratios of *Anderson and Sarmiento* [1994] are used, where P:N:C:O = 1:16:117:−170, yielding R$_{C:O}$ = −0.69, R$_{N:O}$ = −0.094, and R$_{C:N}$ = 7.31. The third term on the right-hand side of equations (A1) and (A2) reflects the changes in DIC caused by dissolution of calcium carbonates. In the dissolution process, the alkalinity will increase twofold faster than increase in inorganic carbon due to release of divalent carbonate ions, CO$_3^{2-}$. This term is adjusted for the decrease in alkalinity associated with increases in nitrate from remineralization of organic material [*Brewer*, 1978]. All

quantities are corrected for changes in salinity over the time period by normalizing to salinities of $t_2$: $nX_{t1} = S_{t2}/ S_{t1}\, X_{t1}$.

[51] Basin-wide, there are no systematic decadal changes in alkalinity (M. Chanson et al., unpublished manuscript, 2010), but small regional changes in alkalinity, often correlated with salinity anomalies, are accounted for in this method. For this method to provide reliable estimates of $\Delta$C$_{anthro}$, it must be assumed that the stoichiometric ratios are correct and invariant. Moreover, movement of boundaries of water masses can lead to anomalous $\Delta$C$_{anthro}$ estimates, as changes in O$_2$ or NO$_3^-$ resulting from changes in circulation and transport will be attributed to changes in remineralization.

[52] Latitude-depth cross sections for the $\Delta$DIC$_{O2}$ and $\Delta$DIC$_{NO3}$ approaches (equations (A1) and (A2)) are shown in Figure A1. There are several known issues with these approaches. *Anderson and Sarmiento* [1994] derived the Redfield ratios from changes in intermediate and deep water in the world's oceans assuming two-end-member mixing. They excluded the North Atlantic because of multi-end-member mixing in this region, and because the ratios did not appear to be constant, either because of issues with the separation of end-members or because the remineralization ratios are variable. In addition, both oxygen and nitrate have limitations as remineralization parameters. Oxygen levels change both due to remineralization and changes in ventilation processes that cannot a priori be separated [*Levine et al.*, 2008]. Nitrogen fixation [*Hansell et al.*, 2007] and possibly denitrification signals advected from the coastal margins, for which nitrate levels are not in Redfield proportions to DIC, can bias the $\Delta$DIC$_{NO3}$ approach. Since there were no absolute standards or certified reference materials for nitrate, biases between cruises that are amplified by the R$_{C:N}$ of 7.31 can affect the results as well. Phosphate (PO$_4$) is, in principle, a good remineralization tracer, as it is not affected by gas exchange or non-Redfieldian decomposition, but the amplification of uncertainty due to the large R$_{C: P}$ of 117, along with poor accuracy of PO$_4$ on some of the cruises, makes this parameter unsuitable for both the remineralization and MLR methods for detecting $\Delta$C$_{anthro}$ on decadal time scales.

[53] The $\Delta$DIC$_{O2}$ and $\Delta$DIC$_{NO3}$ approaches implicitly rely on stationary water masses, as the decadal comparison assumes that the preformed ratios of carbon and nutrients at a particular location do not change over time. On large scales, these are probably reasonable assumptions but in frontal regions this can lead to regional biases. Vertical heave can also introduce biases [e.g., *Rodgers et al.*, 2009]. The movement of fronts often shows up as large negative $\Delta$C$_{anthro}$ anomalies adjacent to positive values. Figure A1a shows a banded pattern of $\Delta$DIC$_{O2}$. This suggests that the changes are related to oceanographic features with vertical structure, such as those associated eddies, Rossby wave and movement of fronts, that affect the patterns of $\Delta$DIC$_{O2}$. Some changes can be attributed to changes in ventilation. The most obvious anomaly is the region of negative $\Delta$DIC$_{O2}$ at 40–55°N that corresponds to the areas with large O$_2$ decreases between 1993 and 2003 (Figure 3b) [*Johnson et al.*, 2005; *Johnson and Gruber*, 2007]. Other regions of negative $\Delta$DIC$_{O2}$ are in the Southern Hemisphere near 46° and at 38°. The latter is associated with a large eddy [*Wanninkhof et al.*, 2006]. The remainder of the region
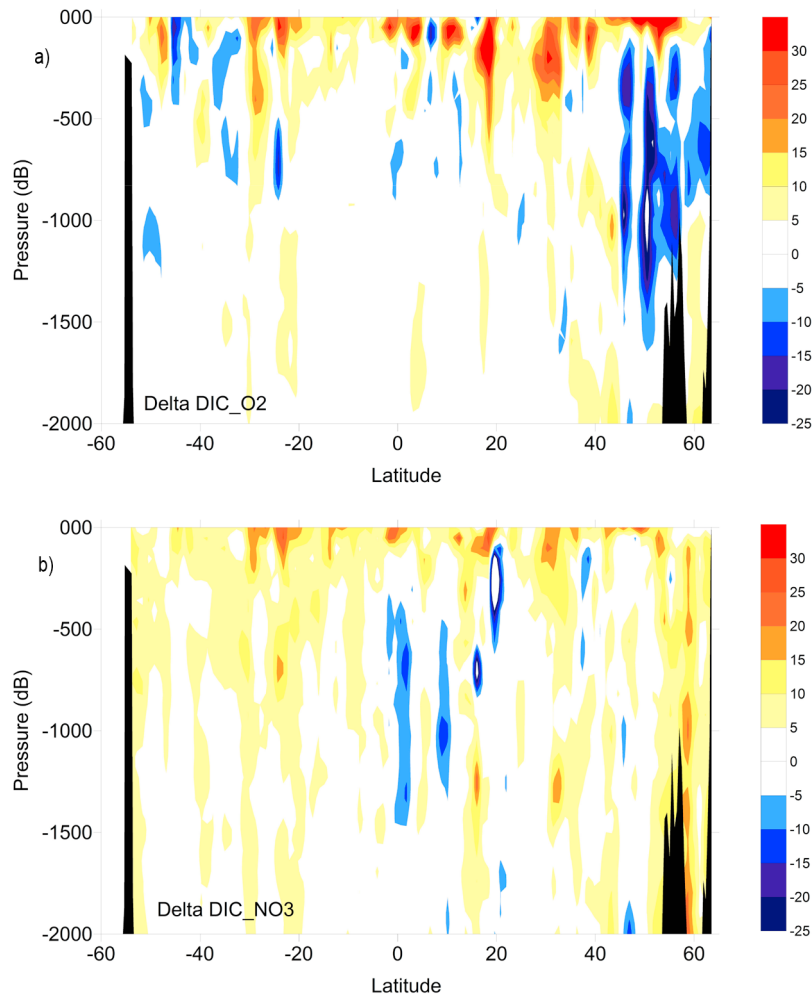
**Figure A1.** Estimated DIC$_{\text{anthro}}$ distributions for the A16 transect computed from the temporal difference in DIC, $\Delta$DIC, for the A16 transect corrected for differences in remineralization using (a) O$_2$ ($\Delta$DIC$_{\text{O2}}$ in $\mu$mol kg$^{-1}$) and (b) NO$_3^-$ ($\Delta$DIC$_{\text{NO3}}$ in $\mu$mol kg$^{-1}$). For the Northern Hemisphere (60°N to 2°S) the cruises took place in 1993 and 2003; for the Southern Hemisphere (2°S to 54°S) the cruise occupied the line in 1989 and 2005, but values are normalized to 1 decade by dividing the values in the south by 10/16. The top 2000 dB are shown.

shows generally positive changes but is patchy in nature. Integrating the $\Delta$DIC$_{\text{O2}}$ over the water column and averaging for the A16 line yields a water column inventory specific change of 0.82 mol m$^{-2}$ yr$^{-1}$ that is higher than the simple difference in DIC over the time period ($\Delta$DIC) of 0.58 mol m$^{-2}$ yr$^{-1}$ (Table A1). Moreover, the spatial variability of $\Delta$DIC$_{\text{O2}}$ and $\Delta$DIC is similar in scale and magnitude (see Figures 3c and A1), suggesting that the remineralization correction based on a stoichiometry of C:O of 117: −170 does not adequately reflect the $\Delta$C$_{\text{anthro}}$.

**Table A1.** Comparison of Specific Inventories for the Atlantic Ocean Along the A16 Section (64°N–54°S) in mol m$^{-2}$ yr$^{-1}$

| Method | North Atlantic (>15°N) | Equatorial Atlantic (15°N–15°S) | South Atlantic (>15°S) | Full Section |
|---|---|---|---|---|
| $\Delta$DIC | 0.82 | 0.23 | 0.56 | 0.58 |
| $\Delta$DIC$_{\text{O2}}$ | 0.92 | 0.60 | 0.86 | 0.82 |
| $\Delta$DIC$_{\text{NO3}}$ | 0.59 | −0.28 | 0.66 | 0.39 |
| $\Delta$DIC$_{\text{eMLR}}$ | 0.59 | 0.68 | 0.78 | 0.68 |
| $\Delta$DIC$_{\text{eMLR-sectional}}$ | 0.69 | 0.17 | 0.96 | 0.65 |
| $\Delta$DIC$_{\text{eMLRdens}}$ | 0.57 | 0.20 | 0.76 | 0.53 |
| $\Delta$DIC$_{\text{C-13}}$[a] | 0.63 ± 0.16 | | | |
| $\Delta$DIC[b] | | | 0.71 ± 0.1 | |

[a]From *Quay et al.* [2007].
[b]From *Murata et al.* [2008]: From the zonal A10 cruise along 30°S, between 35°W and 15°W, 1993–2003 [see *Murata et al.*, 2008, Table 3].

[54] The $\Delta DIC_{NO3}$ shows large regions of decrease near 20°N, 10°N, and the equator (Figure A1b). These decreases correspond with increases in $NO_3^-$ for these regions (not shown) between the occupations in 1993 and 2003. There is no clear attribution for this pattern, and we believe it could be caused by station to station measurement biases during the cruises or changes in circulation patterns in the complex equatorial Atlantic current regime. The negative $\Delta DIC_{O2}$ at 40–55°N is not apparent in the $\Delta DIC_{NO3}$ field. Rather, it shows $\Delta DIC_{NO3}$ increases in the range of 5 to 10 $\mu mol\ kg^{-1}$ that can be attributed to expected ingrowth of $\Delta C_{anthro}$ over time in this well-ventilated region. This points toward a ventilation bias in $\Delta DIC_{O2}$ in this locale. The specific change in $\Delta DIC_{NO3}$ for the whole section of 0.39 mol $m^{-2}$ $yr^{-1}$ is less than the average $\Delta DIC$ value of 0.58 mol $m^{-2}$ $yr^{-1}$ with the major difference in the tropics, 15°N–15°S (Table A1). The large absolute and regional differences between $\Delta DIC_{NO3}$, $\Delta DIC_{O2}$, and $\Delta DIC$ clearly show the large effect of the remineralization correction on the calculation of $\Delta C_{anthro}$, and should serve as a caution using this approach to estimate decadal changes of anthropogenic $CO_2$ in the Atlantic Ocean.

[55] The MLR and eMLR approaches assume that the independent variables are not affected by systematic trends, such as those caused by climate change, or at least not affected in a way that would alter their relationship among each other. The eMLR method gives a much smoother pattern for the change in DIC attributable to $\Delta C_{anthro}$ than the MLR method. This is because the eMLR depends only on the absolute values of the independent variables, which have small relative errors. Different independent variables can be chosen based on personal preference, goodness of fit, linearity, data quality, and data availability. Here we assess the effects of performing the MLR and eMLR for the whole basin and for select latitude bands. A separate MLR analysis of this same data set but using different independent variables is presented by Chanson et al. (unpublished manuscript, 2010) with emphasis on the decadal changes in the coefficients and goodness of fit.

[56] Several different multilinear regression (MLR) approaches are applied to the data set to show the sensitivity of the method to different assumptions. For these comparisons, the DIC was regressed against T, S, AOU, $NO_3^-$, and $SiO_2$ in all approaches. Contrary to the $eMLR_{dens}$ analysis, data in the top 250 m are not used in developing the regressions to avoid biases due to seasonality. Including the top 250 m increases the residuals by up to twofold (from $\approx$ 4–5 $\mu mol$ $kg^{-1}$ to 8–10 $\mu mol\ kg^{-1}$). The MLRs are created with either the 2003 and 2005 data or the 1989 and 1993 data. While the difference in time of occupation of the northern and southern sections could affect the MLR, no apparent biases were found when checked against MLRs created for each section separately. The approaches used are: the single MLR method utilizing the 1989/1993 data (equation (1), main text) to create the regressions and applying the regressions to the newer 2003/2005 data (equation (2), main text); the eMLR method (equation (4)); and the eMLR method applied separately to six latitude intervals (56 to 40°S; 40 to 15°S; 15 to 2°S; 2°S to 15°N; 15 to 40°N; and 40 to 63°N).

[57] The single MLR utilizing the 1989/1993 data to create the regressions and applying the regressions to the newer 2003/2005 data show $\Delta C_{anthro}$ increases of 5 to 10 $\mu mol\ kg^{-1}$ centered at a depth of about 1000 to 1500 m in the North Atlantic and South Atlantic (Figure A2a). There is little change in the near-surface ($\approx$250–500 m) waters of the subtropical gyres. A large area with decreases of 5 to 10 $\mu mol\ kg^{-1}$ is apparent in the intermediate waters from 35°S to 20°N. There are increases of 5 to 10 $\mu mol\ kg^{-1}$ in the deep water. The unanticipated negative changes, and the increases in the deep water, are indicative of biases in the single MLR method that are, in part, attributed to lower data quality of the older data used to create the MLR. This is apparent in Figure A2b where the MLR are created with the 2003/2005 data and used to compare with the 1989/1993 data. In this analysis, the negative values in the intermediate water disappear. Higher $\Delta C_{anthro}$ are found near the surface with a maximum in the upper waters of the South Atlantic. There are also elevated values of 2 to 4 $\mu mol\ kg^{-1}$ in the Antarctic Bottom Water (AABW) that might be attributable to rapid ventilation. However, there are also large negative anomalies at intermediate depths and in the bottom waters in the north that are clearly artifacts, putting the singe-MLR approach for the basin as a whole in doubt. The single MLR method can be refined by computing regressions separately for subbasin regions [Levine et al., 2008].

[58] The eMLR approach (Figure A2c) shows smoother spatial patterns as would be expected by subtracting two linear regressions. The range of temporal changes is smaller, and the patterns of change in $\Delta C_{anthro}$ differ as well compared to the MLR and $DIC_{O2}$ approaches. The spatial patterns are more uniform with highest levels near the surface and decreasing to zero by 2000 m. Near-surface values of 4–5 $\mu mol\ kg^{-1}$ are lower than expected if the ocean uptake were to keep pace with atmospheric increases. No negative values are encountered, indicating that the biases in the single MLRs (Figures A2a and A2b) cancel out. Elevated levels are apparent in the AABW water at high southern latitudes, with values of 3 to 4 $\mu mol\ kg^{-1}$. While this is a ventilation pathway as shown by elevated CFC concentrations, the magnitude of change is large for these depths. These waters are characterized by high silica and nutrient concentrations and this might contribute to the bias of higher $\Delta C_{anthro}$ in these waters using the eMLR.

[59] To determine if there are significant regional (or cruise differences) introduced by the MLR methods, separate MLRs were created for different sections roughly delineating subpolar, subtropical, and tropical gyres: 56 to 40°S; 40 to 15°S; 15 to 2°S; 2°S to 15°N; 15 to 40°N; and 40 to 63°N. The tropical region is split into two sections to separate the northern and southern cruises that occurred in different years. The sectional eMLR ($eMLR_{sectional}$) (Figure A2d) shows truncated $\Delta C_{anthro}$ values for AABW, with no penetration northward of 15°S, likely because of the separate regressions that are created for each region. However, no other large changes in the $\Delta C_{anthro}$ estimate due to truncating the eMLR at each regional boundary are apparent. The $eMLR_{sectional}$ shows higher values at depth at high latitudes and higher values in the subtropics than the eMLR for the whole section (Figures A2c and A2d). The sectional eMLR shows little change in $\Delta C_{anthro}$ in the tropical region and subpolar North Atlantic between 250 and 1000 m (Figure A2d).

[60] Biases in the MLR approaches are assessed from the spatial patterns of the residuals between the measured DIC and the calculated DIC, f(S, T, $SiO_2$, AOU, and $NO_3^-$), for
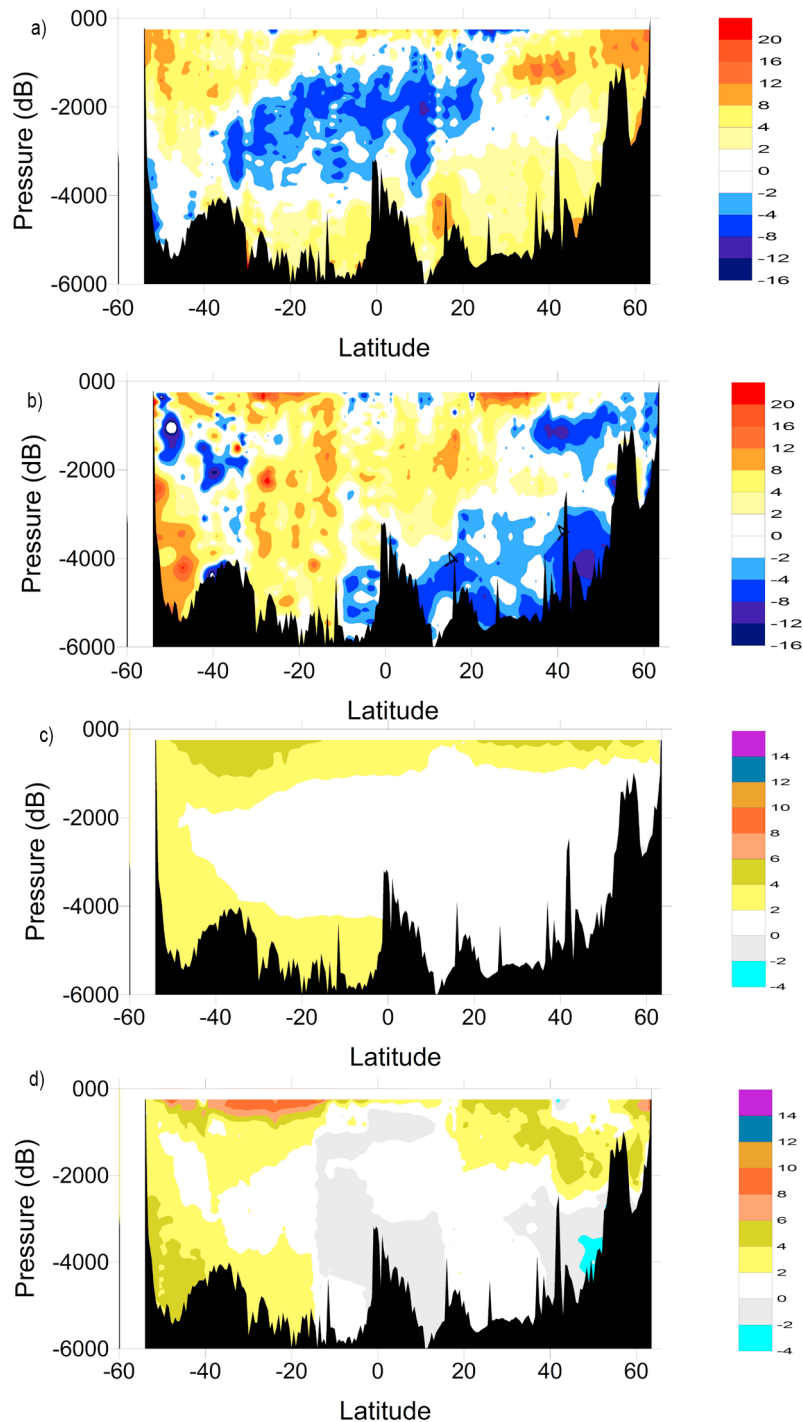
**Figure A2.** Estimated DIC$_{anthro}$ distributions for the A16 transect computed from different multilinear regression (MLR) approaches utilizing S, T, AOU, NO$_3^-$, and SiO$_2$ as input parameters. (a) MLR determined from 1989/1993 data subtracted from 2003/2005 DIC data; (b) 1989/1993 DIC data subtracted from a MLR created from 2003/2005 data; and (c) MLR determined from 1989/1993 data subtracted from the MLR determined with the 2003/2005 data using S, T, AOU, NO$_3^-$, and SiO$_2$ from 2003/2005. The approach is referred to as the extended multilinear regression (eMLR). (d) Difference in DIC for the cruises estimated by the eMLR approach ($\Delta$DIC$_{eMLR}$) with separate MLRs determined for six different latitude ranges ($\Delta$DIC$_{eMLRsectional}$).

the same time period. Contour plots of the residuals are shown in Figures A3a–A3f. The spatial structure in the residuals is nonrandom, which will affect the application of the MLRs to estimate $\Delta$C$_{anthro}$. Moreover, correlations between the independent variables can lead to biases. The whole section of MLRs show the same pattern of spatial

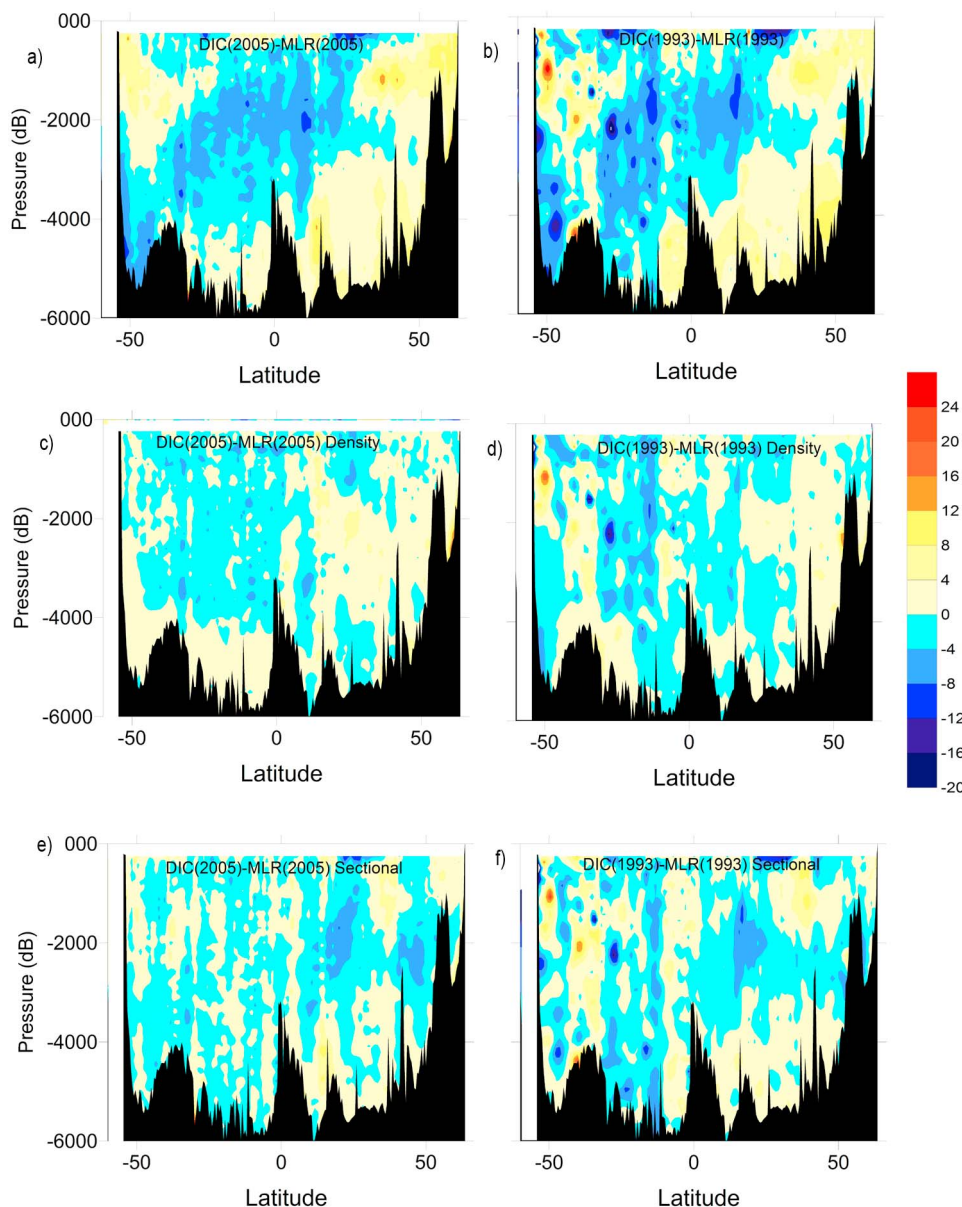**Figure A3.** Biases in the different MLR approaches for estimating DIC distributions. (a) DIC of 2003/2005 − MLR created from 2003/2005 data; (b) DIC of 1989/1993 − MLR created from 1989/1993 data; (c) DIC of 2003/2005 − MLR$_{dens}$ created from 2003/2005 data; (d) DIC of 1989/1993 − MLR$_{dens}$ created from 1989/1993 data; (e) DIC of 2003/2005 − MLR$_{sectional}$ created from 2003/2005 data; and (f) DIC of 1989/1993 − MLR$_{sectional}$ created from 1989/1993 data.

biases whether 1993 or 2005 data are used to create the MLR, but the MLR created with 1993 data show slightly greater magnitudes of biases (compare Figures A3a and A3b). The 2005 residuals are about a half of those of the 1993 data. In both cases, the high latitudes and deep waters in the Northern Hemisphere show positive biases of 4–12 $\mu$mol kg$^{-1}$ while intermediate water and subtropical surface waters show a negative bias of similar magnitude. The eMLR approaches cancel out much of the residual structure. Using a sectional eMLR in which the transect was divided into six latitude bands yields smaller residuals (eMLR$_{sectional}$) (Figures A3e and A3f). The patterns are more horizontal and change sign at the boundaries of the

area with specific MLR. The MLR$_{dens}$, discussed in the main text, show the smallest residuals with values of less than 4 $\mu$mol kg$^{-1}$ (Table 3 and Figures A3c and A3d). There are no clear patterns in the residuals, although the Southern Hemisphere shows predominantly small negative biases and the Northern Hemisphere shows positive offsets at depth.

[61] A comparison of specific inventory estimates for the whole section, and for the North Atlantic, equatorial Atlantic, and South Atlantic sections is provided in Table A1. The changes are normalized to mol m$^{-2}$ yr$^{-1}$ to account for the different times of occupation. A factor of two difference in specific inventories is obtained for the different methods,
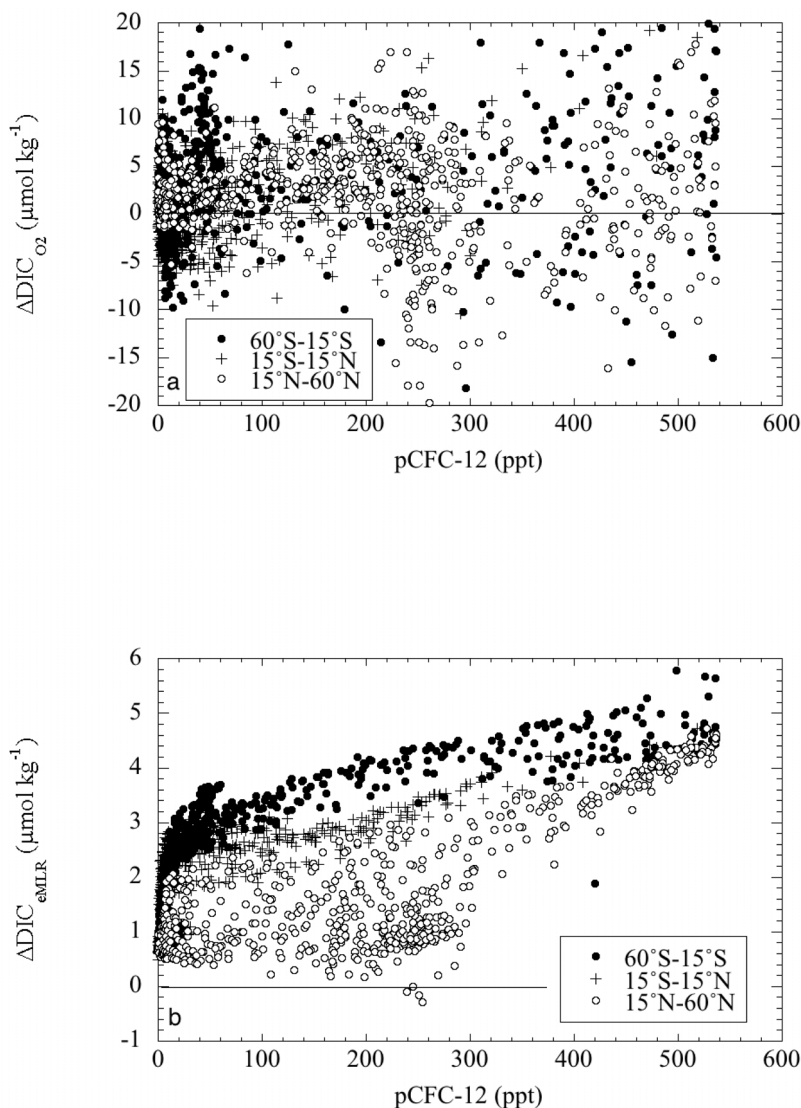
**Figure A4.** Estimates of $\Delta C_{anthro}$ versus pCFC-12. (a) $\Delta DIC_{O2}$ versus pCFC-12 and (b) $\Delta DIC_{eMLR}$ versus pCFC-12 for the depth range of 200–2500 dB. The solid circles are for samples from 60°S to 15°S, the plus symbols are those from 15°S to 15°N, and the open circles are those from 15°N to 60°N. The corresponding plot for $\Delta DIC_{eMLRdens}$ versus pCFC is shown in Figure 6. Note the different scales used for the $\Delta C_{anthro}$ in the panels.

largely due to regional differences between the different methods, particularly in the equatorial Atlantic. In the subtropical gyres in the North and South Atlantic, there is better correspondence between methods. The high $\Delta DIC_{O2}$ values suggest that either the Redfield C:O ratios used are too high for the North Atlantic [*Li and Peng*, 2002], or, more likely, that the net decrease of O$_2$ in the North Atlantic thermocline in the 1990s biases the $\Delta C_{anthro}$ estimate determined by $\Delta DIC_{O2}$. This is in accord with observations of *Keeling and Garcia* [2002]. *Levine et al.* [2008] similarly find, using a numerical model, that changes in O$_2$ due to ventilation and mixing significantly affect estimates of $\Delta C_{anthro}$ using the $\Delta DIC_{O2}$ method. The lower values using the $\Delta DIC_{NO3}$, particularly in the tropics, are attributed to biases in NO$_3^-$ data or changes in currents.

[62] A further check of the different methods to estimate $\Delta C_{anthro}$ can be performed by comparison with pCFCs. The

$\Delta DIC_{O2}$ method shows no apparent trend with pCFC and gives a wide range of values (Figure A4a). The $\Delta DIC_{NO3}$ method has a similar random distribution (not shown). The $\Delta DIC_{eMLR}$ (Figure A4b) shows distinct, but different relationships between increasing anthropogenic carbon and pCFC for different regions. For the South Atlantic, a near-linear increase in $\Delta DIC_{eMLR}$ with pCFC is observed. The waters in the Northern Hemisphere show two diverging trends. All waters between $\approx$ 200–500 db from 15 to 40°N, and the entire water column from 40 to 60°N, show a clear positive slope between $\Delta DIC_{eMLR}$ and pCFC. The deeper waters between 15°N to 40°N show approximately constant $\Delta DIC_{eMLR}$ of $\approx$ 1 $\mu$mol kg$^{-1}$ for pCFC-12 varying from 0 to 250 ppt. This is because the pCFC decreases along isopycnal surfaces into the interior while the $\Delta DIC_{eMLR}$ as applied is a basin-wide regression that does not necessarily account for the pathways of transport. The data in the

equatorial area lie between the northern and southern relationships, likely because the deeper water masses in this region do not form locally but are mixtures of northern and southern component waters.

[63] The comparison of methods show large differences in $\Delta C_{anthro}$ for the whole section and, particularly, regionally. The methods show inconsistencies with respect to the residuals and when comparing the magnitudes with pCFC that cast doubt on the accuracy of the approaches. A rigorous set of diagnostics should be applied before inferring the $\Delta C_{anthro}$ from the approaches applied. The eMLR$_{dens}$ approach discussed in the main text appears the most robust empirical approach of determining decadal changes of anthropogenic CO$_2$ for the meridional section A16 in the Atlantic.

# References

Anderson, L. A., and J. L. Sarmiento (1994), Redfield ratios of remineralization determined by nutrient data analysis, *Global Biogeochem. Cycles*, 8, 65–80, doi:10.1029/93GB03318.

Bates, N. R. (2007), Interannual variability of the oceanic CO$_2$ sink in the subtropical gyre of the North Atlantic Ocean over the last 2 decades, *J. Geophys. Res.*, 112, C09013, doi:10.1029/2006JC003759.

Bates, N. R., A. C. Pequignet, R. J. Johnson, and N. Gruber (2002), Changes in the oceanic sink of CO$_2$ in Subtropical Mode Water of the North Atlantic Ocean, *Nature*, 420, 489–493, doi:10.1038/nature01253.

Belkin, I. M. (2004), Propagation of the "Great Salinity Anomaly" of the 1990s around the northern North Atlantic, *Geophys. Res. Lett.*, 31, L08306, doi:10.1029/2003GL019334.

Brewer, P. G. (1978), Direct observation of the oceanic CO$_2$ increase, *Geophys. Res. Lett.*, 5, 997–1000, doi:10.1029/GL005i012p00997.

Brewer, P. G., C. Goyet, and G. Friederich (1997), Direct observation of the oceanic CO$_2$ increase revisited, *Proc. Natl. Acad. Sci. U. S. A.*, 94, 8308–8313, doi:10.1073/pnas.94.16.8308.

Brix, H., N. Gruber, and C. D. Keeling (2004), Interannual variability in the upper ocean carbon cycle at Station ALOHA, Hawaii, *Global Biogeochem. Cycles*, 18, GB4019, doi:10.1029/2004GB002245.

Broecker, W. S., and H. G. Östlund (1979), Property distributions along the sigma theta = 26.8 isopycnal in the Atlantic Ocean, *J. Geophys. Res.*, 84, 1145–1154, doi:10.1029/JC084iC03p01145.

Broecker, W. S., and T.-H. Peng (1982), *Tracers in the Sea*, Eldigio, Palisades, N. Y.

Brown, P. J., D. C. E. Bakker, U. Schuster, and A. J. Watson (2010), Anthropogenic carbon accumulation in the subtropical North Atlantic, *J. Geophys. Res.*, 115, C04016, doi:10.1029/2008JC005043.

Castle, R., R. Wanninkhof, S. C. Doney, J. Bullister, L. Johns, R. A. Feely, B. E. Huss, F. J. Millero, and K. Lee (1998), Chemical and hydrographic profiles and underway measurements from the North Atlantic during July and August of 1993, *NOAA Data Rep., ERL AOML-32*, Atl. Oceanogr. and Meteorol. Lab., NOAA, Miami, Fla.

Chen, C.-T., and F. J. Millero (1979), Gradual increase of oceanic CO$_2$, *Nature*, 277, 205–206, doi:10.1038/277205a0.

Chung, S.-N., K. Lee, R. A. Feely, C. L. Sabine, F. J. Millero, R. Wanninkhof, R. M. Key, J. L. Bullister, and T.-H. Peng (2003), Calcium carbonate budget in the Atlantic Ocean based on water column inorganic carbon chemistry, *Global Biogeochem. Cycles*, 17(4), 1093, doi:10.1029/2002GB002001.

Crutzen, P. J., and W. Steffen (2003), How long have we been in the Anthropocene era?, *Clim. Change*, 61, 251–257, doi:10.1023/B:CLIM.0000004708.74871.62.

Curry, R. G., and C. Mauritzen (2005), Dilution of the northern North Atlantic Ocean in recent decades, *Science*, 308, 1772–1774, doi:10.1126/science.1109477.

Doney, S. C., and J. L. Bullister (1992), A chlorofluorocarbon section in the eastern North Atlantic, *Deep Sea Res.*, 39, 1857–1883, doi:10.1016/0198-0149(92)90003-C.

Doney, S. C., W. J. Jenkins, and J. L. Bullister (1997), A comparison of ocean tracer dating techniques on a meridional section in the eastern North Atlantic, *Deep Sea Res., Part I*, 44, 603–626, doi:10.1016/S0967-0637(96)00105-7.

Doney, S. C., J. L. Bullister, and R. Wanninkhof (1998), Climatic variability in ocean ventilation rates diagnosed using chlorofluorocarbons, *Geophys. Res. Lett.*, 25, 1399–1402, doi:10.1029/98GL00844.

Doney, S. C., K. Lindsay, I. Fung, and J. John (2006), Natural variability in a stable, 1000-yr global coupled climate-carbon cycle simulation, *J. Clim.*, 19, 3033–3054, doi:10.1175/JCLI3783.1.

Doney, S. C., S. Yeager, G. Danabasoglu, W. G. Large, and J. C. McWilliams (2007), Mechanisms governing interannual variability of upper ocean temperature in a global hindcast simulation, *J. Phys. Oceanogr.*, 37, 1918–1938, doi:10.1175/JPO3089.1.

Doney, S. C., I. Lima, J. K. Moore, K. Lindsay, M. J. Behrenfeld, T. K. Westberry, N. Mahowald, D. M. Glover, and T. Takahashi (2009), Skill metrics for confronting global upper ocean ecosystem-biogeochemistry models against field and remote sensing data, *J. Mar. Syst.*, 76, 95–112, doi:10.1016/j.jmarsys.2008.05.015.

Dore, J. E., R. Lukas, D. W. Sadler, and D. M. Karl (2003), Climate-driven changes to the atmospheric CO$_2$ sink in the subtropical North Pacific Ocean, *Nature*, 424, 754–757, doi:10.1038/nature01885.

Emerson, S., S. Mecking, and J. Abell (2001), The biological pump in the subtropical North Pacific Ocean: Nutrient sources, Redfield ratios, and recent changes, *Global Biogeochem. Cycles*, 15, 535–554, doi:10.1029/2000GB001320.

Friedlingstein, P., et al. (2006), Climate-carbon cycle feedback analysis: Results from the (CMIP)-M-4 model intercomparison, *J. Clim.*, 19, 3337–3353, doi:10.1175/JCLI3800.1.

Friis, K., A. Körtzinger, J. Patsch, and D. W. R. Wallace (2005), On the temporal increase of anthropogenic CO$_2$ in the subpolar North Atlantic, *Deep Sea Res., Part I*, 52, 681–698, doi:10.1016/j.dsr.2004.11.017.

Garzoli, S., et al. (2010), Progressing towards global sustained deep ocean observations, in *OceanObs'09: Sustained Ocean Observations and Information for Society*, edited by J. Hall et al., *ESA Publ.*, WPP-306, 12 pp.

Gouretski, V. V., and K. Jancke (2000), Systematic errors as the cause for an apparent deep water property variability: Global analysis of the WOCE and historical hydrographic data, *Prog. Oceanogr.*, 48, 337–402, doi:10.1016/S0079-6611(00)00049-5.

Gruber, N. (1998), Anthropogenic CO$_2$ in the Atlantic Ocean, *Global Biogeochem. Cycles*, 12, 165–191, doi:10.1029/97GB03658.

Gruber, N., and J. L. Sarmiento (2002), Biogeochemical/physical interactions in elemental cycles, in *The Sea: Biological-Physical Interactions in the Oceans*, edited by A. R. Robinson et al., pp. 337–399, John Wiley, Hoboken, N. J.

Gruber, N., J. L. Sarmiento, and T. F. Stocker (1996), An improved method for detecting anthropogenic CO$_2$ in the oceans, *Global Biogeochem. Cycles*, 10, 809–837, doi:10.1029/96GB01608.

Gruber, N., C. D. Keeling, and N. R. Bates (2002), Interannual variability in the North Atlantic ocean carbon sink, *Science*, 298, 2374–2378, doi:10.1126/science.1077077.

Hansell, D. A., D. Olson, F. Dentener, and L. Zamora (2007), Assessment of excess nitrate development in the subtropical North Atlantic, *Mar. Chem.*, 106, 562–579, doi:10.1016/j.marchem.2007.06.005.

Intergovernmental Oceanographic Commission (2009), Ship-based repeat hydrography: A strategy for a sustained global program, *IOC Tech. Ser. 89*, U.N. Educ., Sci., and Cult. Organ., Paris.

Johnson, G. C., and S. C. Doney (2006), Recent western South Atlantic bottom water warming, *Geophys. Res. Lett.*, 33, L14614, doi:10.1029/2006GL026769.

Johnson, G. C., and N. Gruber (2007), Decadal water mass variations along 20°W in the northeastern Atlantic Ocean, *Prog. Oceanogr.*, 73, 277–295, doi:10.1016/j.pocean.2006.03.022.

Johnson, G. C., J. L. Bullister, and N. Gruber (2005), Labrador Sea Water property variations in the northeastern Atlantic Ocean, *Geophys. Res. Lett.*, 32, L07602, doi:10.1029/2005GL022404.

Joos, F., G.-K. Plattner, T. F. Stocker, O. Marchal, and A. Schmittner (1999), Global warming and marine carbon cycle feedbacks on future atmospheric CO$_2$, *Science*, 284, 464–467, doi:10.1126/science.284.5413.464.

Kawase, M., and J. L. Sarmiento (1985), Nutrients in the Atlantic thermocline, *J. Geophys. Res.*, 90, 8961–8979, doi:10.1029/JC090iC05p08961.

Keeling, R., and H. E. Garcia (2002), The change in oceanic $O_2$ inventory associated with recent global warming, *Proc. Natl. Acad. Sci. U. S. A.*, 99, 7848–7853.

Keeling, C. D., H. Brix, and N. Gruber (2004), Seasonal and long-term dynamics of the upper ocean carbon cycle at Station ALOHA near Hawaii, *Global Biogeochem. Cycles*, 18, GB4006, doi:10.1029/2004GB002227.

Key, R. M., A. Kozyr, C. L. Sabine, K. Lee, R. Wanninkhof, J. L. Bullister, R. A. Feely, F. J. Millero, C. Mordy, and T. H. Peng (2004), A global ocean carbon climatology: Results from Global Data Analysis Project (GLODAP), *Global Biogeochem. Cycles*, 18, GB4031, doi:10.1029/2004GB002247.

Key, R. M., et al. (2010), The CARINA data synthesis project: Introduction and overview, *Earth Syst. Sci. Data*, 2, 105–121, doi:10.5194/essd-2-105-2010.

Khatiwala, S., F. Primeau, and T. Hall (2009), Reconstruction of the history of anthropogenic $CO_2$ concentrations in the ocean, *Nature*, 462, 346–349, doi:10.1038/nature08526.

Körtzinger, A., M. Rhein, and L. Mintrop (1999), Anthropogenic $CO_2$ and CFCs in the North Atlantic Ocean—A comparison of man-made tracers, *Geophys. Res. Lett.*, 26, 2065–2068, doi:10.1029/1999GL900432.

Lee, K., F. J. Millero, and R. Wanninkhof (1997), The carbon dioxide system in the Atlantic Ocean, *J. Geophys. Res.*, 102, 15,693–15,707, doi:10.1029/97JC00067.

Lee, K., S.-D. Choi, G.-H. Park, R. Wanninkhof, T.-H. Peng, R. M. Key, C. L. Sabine, R. A. Feely, J. L. Bullister, and F. J. Millero (2003), An updated anthropogenic $CO_2$ inventory in the Atlantic Ocean, *Global Biogeochem. Cycles*, 17(4), 1116, doi:10.1029/2003GB002067.

Le Quéré, C., et al. (2007), Saturation of the Southern Ocean $CO_2$ sink due to recent climate change, *Science*, 316, 1735–1738, doi:10.1126/science.1136188.

Le Quéré, C., et al. (2009), Trends in the sources and sinks of carbon dioxide, *Nat. Geosci.*, 2, 831–836, doi:10.1038/ngeo689.

Levine, N. M., S. C. Doney, R. Wanninkhof, K. Lindsay, and I. Y. Fung (2008), The impact of ocean carbon system variability on the detection of temporal increases in anthropogenic $CO_2$, *J. Geophys. Res.*, 113, C03019, doi:10.1029/2007JC004153.

Li, Y.-H., and T.-H. Peng (2002), Latitudinal change of remineralization ratios in the oceans and its implication for nutrient cycles, *Global Biogeochem. Cycles*, 16(4), 1130, doi:10.1029/2001GB001828.

Lo Monaco, C., N. Metzl, A. Poisson, C. Brunet, and B. Schauer (2005), Anthropogenic $CO_2$ in the Southern Ocean: Distribution and inventory at the Indian-Atlantic boundary (World Ocean Circulation Experiment line I6), *J. Geophys. Res.*, 110, C06010, doi:10.1029/2004JC002643.

Lovenduski, N. S., N. Gruber, S. C. Doney, and I. D. Lima (2007), Enhanced $CO_2$ outgassing in the Southern Ocean from a positive phase of the Southern Annular Mode, *Global Biogeochem. Cycles*, 21, GB2026, doi:10.1029/2006GB002900.

Lovenduski, N. S., N. Gruber, and S. C. Doney (2008), Toward a mechanistic understanding of the decadal trends in the Southern Ocean carbon sink, *Global Biogeochem. Cycles*, 22, GB3016, doi:10.1029/2007GB003139.

Marengo, J. A., C. A. Nobre, J. Tomasella, M. D. Oyama, G. S. De Oliveira, R. De Oliveira, H. Camargo, L. M. Alves, and I. F. Brown (2008), The drought of Amazonia in 2005, *J. Clim.*, 21, 495–516, doi:10.1175/2007JCLI1600.1.

Matear, R. J., T. A. Hirst, and B. I. McNeil (2000), Changes in dissolved oxygen in the Southern Ocean with climate change, *Geochem. Geophys. Geosyst.*, 1(11), 1050, doi:10.1029/2000GC000086.

Matsumoto, K., and N. Gruber (2005), How accurate is the estimation of anthropogenic carbon in the ocean? An evaluation of the $\Delta C^*$ method, *Global Biogeochem. Cycles*, 19, GB3014, doi:10.1029/2004GB002397.

McNeil, B. I., R. J. Matear, R. M. Key, J. L. Bullister, and J. L. Sarmiento (2003), Anthropogenic $CO_2$ uptake by the ocean using the global chlorofluorocarbon dataset, *Science*, 299, 235–239, doi:10.1126/science.1077429.

Mikaloff Fletcher, S. E., et al. (2006), Inverse estimates of anthropogenic $CO_2$ uptake, transport, and storage by the ocean, *Global Biogeochem. Cycles*, 20, GB2002, doi:10.1029/2005GB002530.

Murata, A., Y. Kumamoto, K. Sasaki, S. Watanabe, and M. Fukasawa (2008), Decadal increases of anthropogenic $CO_2$ in the subtropical South Atlantic Ocean along 30°S, *J. Geophys. Res.*, 113, C06007, doi:10.1029/2007JC004424.

Peng, T.-H., and R. Wanninkhof (2010), Increase of anthropogenic $CO_2$ in the Atlantic Ocean in last the two decades, *Deep Sea Res., Part I*, 57, 755–770, doi:10.1016/j.dsr.2010.03.008.

Peng, T.-H., R. Wanninkhof, and R. A. Feely (2003), Increase of anthropogenic $CO_2$ in the Pacific Ocean over the last two decades, *Deep Sea Res., Part II*, 50, 3065–3082, doi:10.1016/j.dsr2.2003.09.001.

Pérez, F. F., M. Vázquez-Rodríguez, E. Louarn, X. A. Padín, H. Mercier, and A. F. Ríos (2008), Temporal variability of the anthropogenic $CO_2$ storage in the Irminger Sea, *Biogeosciences*, 5, 1669–1679, doi:10.5194/bg-5-1669-2008.

Plattner, G.-K., et al. (2008), Long-term climate commitments projected with climate carbon cycle models, *J. Clim.*, 21, 2721–2751, doi:10.1175/2007JCLI1905.1.

Quay, P., R. Sonnerup, J. Stutsman, J. Maurer, A. Körtzinger, X. A. Padin, and C. Robinson (2007), Anthropogenic $CO_2$ accumulation rates in the North Atlantic Ocean from changes in the $^{13}C/^{12}C$ of dissolved inorganic carbon, *Global Biogeochem. Cycles*, 21, GB1009, doi:10.1029/2006GB002761.

Rodgers, K. B., et al. (2009), Using altimetry to help explain patchy changes in hydrographic carbon measurements, *J. Geophys. Res.*, 114, C09013, doi:10.1029/2008JC005183.

Sabine, C. L., et al. (2004), The oceanic sink for anthropogenic $CO_2$, *Science*, 305, 367–371, doi:10.1126/science.1097403.

Sabine, C. L., R. A. Feely, F. J. Millero, A. G. Dickson, C. Langdon, S. Mecking, and D. Greeley (2008), Decadal changes in Pacific carbon, *J. Geophys. Res.*, 113, C07021, doi:10.1029/2007JC004577.

Sarmiento, J. L., and N. Gruber (2002), Sinks for anthropogenic carbon, *Phys. Today*, 55(8), 30–36, doi:10.1063/1.1510279.

Sarmiento, J. L., and C. Le Quéré (1996), Oceanic carbon dioxide uptake in a model of century-scale global warming, *Science*, 274, 1346–1350, doi:10.1126/science.274.5291.1346.

Sarmiento, J. L., J. C. Orr, and U. Siegenthaler (1992), A perturbation simulation of $CO_2$ uptake in an ocean general circulation model, *J. Geophys. Res.*, 97, 3621–3645, doi:10.1029/91JC02849.

Sarmiento, J. L., N. Gruber, M. Brzezinski, and J. Dunne (2004), High latitude controls of thermocline nutrients and low latitude biological productivity, *Nature*, 427, 56–60, doi:10.1038/nature02127.

Sarmiento, J. L., J. Simeon, A. Gnanadesikan, N. Gruber, R. M. Key, and R. Schlitzer (2007), Deep-ocean biogeochemistry of silicic acid and nitrate, *Global Biogeochem. Cycles*, 21, GB1S90, doi:10.1029/2006GB002720.

Shulenberger, E., and L. Reid (1981), The Pacific shallow oxygen maximum, deep chlorophyll maximum, and primary production, reconsidered, *Deep Sea Res.*, 28, 901–919, doi:10.1016/0198-0149(81)90009-1.

Solomon, S., et al. (2007), Technical summary, in *Climate Change 2007: The Physical Science Basis—Contribution of Working Group I to the Fourth Assessment Report of the Intergovernmental Panel on Climate Change*, edited by S. Solomon et al., pp. 77–79, Cambridge Univ. Press, Cambridge, U. K.

Stott, P. A., R. T. Sutton, and D. M. Smith (2008), Detection and attribution of Atlantic salinity changes, *Geophys. Res. Lett.*, 35, L21702, doi:10.1029/2008GL035874.

Stramma, L., P. Brandt, J. Schafstall, F. Schott, J. Fischer, and A. Körtzinger (2008), Oxygen minimum zone in the North Atlantic south and east of the Cape Verde Islands, *J. Geophys. Res.*, 113, C04014, doi:10.1029/2007JC004369.

Stramma, L., S. Schmidtko, L. A. Levin, and G. C. Johnson (2010), Ocean oxygen minima expansions and their biological impacts, *Deep Sea Res., Part I*, 57, 587–595, doi:10.1016/j.dsr.2010.01.005.

Tanhua, T., A. Biastoch, A. Körtzinger, H. Lüger, C. Boning, and D. W. R. Wallace (2006), Changes of anthropogenic $CO_2$ and CFCs in the North Atlantic between 1981 and 2004, *Global Biogeochem. Cycles*, 20, GB4017, doi:10.1029/2006GB002695.

Tanhua, T., A. Körtzinger, K. Friis, D. W. Waugh, and D. W. R. Wallace (2007), An estimate of anthropogenic $CO_2$ inventory from decadal changes in oceanic carbon content, *Proc. Natl. Acad. Sci. U. S. A.*, 104, 3037–3042, doi:10.1073/pnas.0606574104.

Thomas, H., A. E. Friederike Prowe, I. D. Lima, S. C. Doney, R. Wanninkhof, R. J. Greatbach, U. Schuster, and A. Corbiere (2008), Changes in the North Atlantic Oscillation influence $CO_2$ uptake in the North Atlantic over the past 2 decades, *Global Biogeochem. Cycles*, 22, GB4027, doi:10.1029/2007GB003167.

Thorpe, S. A. (1984), The role of bubbles produced by breaking waves in super-saturating the near surface mixed layer with oxygen, *Ann. Geophys.*, 2, 53–56.

Touratier, F., and C. Goyet (2004), Applying the new TrOCA approach to estimate the distribution of anthropogenic $CO_2$ in the Atlantic Ocean, *J. Mar. Syst.*, 46, 181–197, doi:10.1016/j.jmarsys.2003.11.020.

Tsuchiya, M., L. D. Talley, and M. S. McCartney (1992), An eastern Atlantic section from Iceland southward across the equator, *Deep Sea Res.*, 39, 1885–1917, doi:10.1016/0198-0149(92)90004-D.

Tsuchiya, M., L. D. Talley, and M. S. McCartney (1994), Water-mass distributions in the western South Atlantic: A section from South Georgia Island (54°S) northward across the equator, *J. Mar. Res.*, 52, 55–81, doi:10.1357/0022240943076759.

U.S. Department of Energy (1994), Handbook of methods for the analysis of the various parameters of the carbon dioxide system in sea water, version 2, *Rep. ORNL/CDIAC-74*, Oak Ridge Natl. Lab., Oak Ridge, Tenn.

Vázquez-Rodríguez, M., F. Touratier, C. Lo Monaco, D. W. Waugh, X. A. Padin, R. G. J. Bellerby, C. Goyet, N. Metzl, A. F. Ríos, and F. F. Pérez (2009), Anthropogenic carbon distributions in the Atlantic Ocean: Data-based estimates from the Arctic to the Antarctic, *Biogeosciences*, 6, 439–451, doi:10.5194/bg-6-439-2009.

Wallace, D. W. R. (2001), Storage and transport of excess CO$_2$ in the oceans: The JGOFS/WOCE global CO$_2$ survey, in *Ocean Circulation and Climate*, edited by G. Siedler et al., pp. 489–521, Academic, San Diego, Calif.

Wallace, D. W. R., P. Beining, and A. Putzka (1994), Carbon-tetrachloride and chlorofluorocarbons in the South Atlantic Ocean, 19°S, *J. Geophys. Res.*, 99, 7803–7819, doi:10.1029/94JC00031.

Wanninkhof, R., and K. Thoning (1993), Measurement of fugacity of CO$_2$ in surface water using continuous and discrete sampling methods, *Mar. Chem.*, 44, 189–204, doi:10.1016/0304-4203(93)90202-Y.

Wanninkhof, R., S. Doney, T.-H. Peng, J. L. Bullister, K. Lee, and R. A. Feely (1999), Comparison of methods to determine the anthropogenic CO$_2$ invasion into the Atlantic Ocean, *Tellus, Ser. B*, 51, 511–530.

Wanninkhof, R., T.-H. Peng, B. Huss, C. L. Sabine, and K. Lee (2003), Comparison of inorganic carbon system parameters measured in the Atlantic Ocean from 1990 to 1998 and recommended adjustments, *Rep. ORNL/CDIAC-140*, Oak Ridge Natl. Lab., Oak Ridge, Tenn.

Wanninkhof, R., S. C. Doney, R. D. Castle, F. J. Millero, J. L. Bullister, D. A. Hansell, M. J. Warner, C. Langdon, G. C. Johnson, and C. W. Mordy (2006), Carbon dioxide, hydrographic and chemical data obtained during the R/V *Ronald H. Brown* repeat hydrography cruise in the Atlantic Ocean: CLIVAR CO$_2$ section A16S_2005, *Rep. RNL/CDIAC-151, NDP-087*, Oak Ridge Natl. Lab., Oak Ridge, Tenn.

Warner, M. J., and R. F. Weiss (1985), Solubilities of chlorofluorocarbons 11 and 12 in water and seawater, *Deep Sea Res.*, 32, 1485–1497, doi:10.1016/0198-0149(85)90099-8.

Watson, A. J., et al. (2009), Tracking the variable North Atlantic sink for atmospheric CO$_2$, *Science*, 326, 1391–1393, doi:10.1126/science.1177394.

Waugh, D. W., T. M. Hall, B. I. McNeil, R. Key, and R. J. Matear (2006), Anthropogenic CO$_2$ in the oceans estimated using transit time distributions, *Tellus, Ser. B*, 58, 376–389.

World Ocean Circulation Experiment (1994), WOCE operations manual, section 3.1: WOCE hydrographic program, 144 pp., Woods Hole, Mass.

Yool, A., A. Oschlies, A. J. G. Nurser, and N. Gruber (2010), A model-based assessment of the TrOCA approach for estimating anthropogenic carbon in the ocean, *Biogeosciences*, 7, 723–751, doi:10.5194/bg-7-723-2010.

J. L. Bullister, Ocean Climate Research Division, PMEL, NOAA, 7600 Sand Point Way NE, Seattle, WA 98115, USA. (john.l.bullister@noaa.gov)

S. C. Doney, Woods Hole Oceanographic Institution, Woods Hole, MA 02543, USA. (sdoney@whoi.edu)

N. Gruber, Environmental Physics, Institute of Biogeochemistry and Pollutant Dynamics, ETH Zurich, CH-8092 Zurich, Switzerland. (nicolas.gruber@env.ethz.ch)

N. M. Levine, OEB Department, Harvard University, Cambridge, MA 02138, USA. (nlevine@oeb.harvard.edu)

R. Wanninkhof, Ocean Chemistry Division, AOML, NOAA, 4301 Rickenbacker Causeway, Miami, FL 33149, USA. (rik.wanninkhof@yahoo.com)

M. Warner, School of Oceanography, University of Washington, Box 357940, Seattle, WA 98195, USA. (warner@u.washington.edu)